University of Nottingham Ningbo China

Department of Mechanical, Materials and Manufacturing Engineering

Mechanical properties of stabilized soils for pavement applications

Mingwei FENG

20219269

THESIS SUBMITTED TO THE UNIVERSITY OF NOTTINGHAM FOR THE DEGREE OF MASTER OF RESEARCH

Abstract

With the continuous development of economy and society, the requirement of road pavement construction is increasing gradually in China. The mining of traditional road fill materials such as sand, stone causes a lot of wastes, which has a negative impact on the environment. Hence, reclaim of wastes has attracted more and more attentions nowadays. Weak waste soils from construction sites or dredging sites can be considered as alternative raw materials for embankment filling after stabilization. The stabilized soil has become one of the new environment-friendly materials which is economic and of good engineering stability to meet the requirement of pavement construction.

The primary objective of this project was to investigate the mechanical properties of stabilized soils for pavement applications. Three types of soils were used in this study. One was a fine soil (silty clay) and the other two were dewatered drilling slurries. By conducting a series of tests, the mechanical properties including unconfined compressive strength, California bearing ratio (CBR), triaxial shear strength, splitting tensile strength and stiffness modulus were investigated. The effects of stabilizer content, moisture content, curing and sampling preparation method and wetting-drying cycles on the mechanical properties of the stabilized soil were studied in a comprehensive manner. From a series of quantitative analyses and grey-correlation analyses, it was found that, among all stabilizers used in this study, cement is the most effective for improving the strength of the stabilized soil. Meanwhile, the moisture content has a significant effect on the strength. On the wet-side of the optimum moisture content, the strength of stabilized soil is decreased when the moisture content is raised. With the increase of the wetting-drying cycles, the strength increases to a peak value and then decreases, which is attributed to a combined effect of the change of the moisture when drying and the change of the internal structure due to the wetting-drying cycles.

Numerical analyses were also conducted considering a pavement structure with a stabilized soil embankment laying on a layered soft subsoil. Settlement of the subsoil was predicted after a multi-stage construction and consolidation. Stress distribution in the embankment was obtained and the results show that the strength of the stabilized soil meets the requirement of the pavement structure. Finally, some engineering implications were

concluded to guide practical pavement constructions.

Contents

List of Figures

List of Tables

List of Equations

Acknowledgements

I would like to express my sincere appreciations and gratitude to Dr. Juan Wang for the invaluable guidance and supports to the Master of Research study. I would also like to express thanks to Dr. Shu Liu and Mr. Peng Chen for their assistance. Working with them provided me with an enriching experience in my academic life. Their encouragements and supports also helped me complete this dissertation.

Notations

CE	-	Cement
FA	-	Fly ash
CA	-	CaO
CAS	-	$CaSO_4$
C	-	Commercial stabilizer
M	-	Moisture content
T	-	Curing age
WD	-	Wetting-drying cycle
W	-	Water soaking
D	-	Drying
R	-	Pre-curing age
L	-	Adding stabilizer later
UCS	-	Unconfined compressive strength
CBR	-	California bearing ratio
OMC	-	Optimum moisture content

Chapter 1: Introduction

1.1 Background

With the continuously development of infrastructure construction in China, the mileage of highways and urban roads is increasing rapidly, which leads to an increasing demand of the filling materials for pavement construction. This would consume a large amount of natural resources and cause damages to the environment. To build a resource-saving and environment-friendly society, the re-utilization of waste materials, such as muck, slurry and construction wastes, in pavement foundation has attracted more attentions these years. For the waste materials with low strength like dredging slurry, they always mix with stabilizers to satisfy the strength requirement as pavement materials. For example, Zhang et al. (2004b) used mucky soil with a moisture content of 65.4% as the embankment materials with an addition of 12% cement. And Cheng et al. (2015) used dredging silt with a moisture content of 89.7% as the embankment materials with additions of 8% cement, 17.5% fly ash, 15% lime and 0.13% high water absorbing resin. However, the high moisture content of waste materials consumes large amount of stabilizers, thus high costs. A pre-treatment on the waste materials in a mechanical manner, such as mechanical dewatering, can reduce the moisture content with low costs and save the dosage of chemical stabilizers. However, the mechanical properties of dewatered soil before and after stabilization and their application in pavement construction need further studies.

1.2 Aims and objectives

This overall purpose of this research is to study the mechanical behaviors of weak soil stabilized by different stabilizers so that they can be used in pavement construction. The effect of some main influencing factors on the strength of the stabilized soil will be assessed experimentally, which can guide the selection of a proper mix formulation and construction method in the practice. Also, numerical studies will be carried out considering a practical case to check the feasibility of the material in reality. The main objectives include:

(1) To study the influence degree and order of different stabilizers on the unconfined

compressive strength of the stabilized soils.

(2) To study the effect of initial moisture content on the strength of the stabilized soil.

(3) To study the effect of curing condition and sampling method on the strength of the stabilized soil to guide the practical construction.

(4) To study the effect of wetting-drying cycles on the strength of the stabilized soil to simulate the effect of climate changing in reality.

(5) To predict the settlement of the subsoil due to the construction of a pavement structure with a stabilized soil embankment and examine if the strength of the stabilized soil meets the requirement of a pavement structure in reality.

1.3 Outline

This thesis is divided into eight chapters, a brief outline is given below:

Chapter 1 introduces the background of the research. The key objectives of this study have also been stated.

Chapter 2 focuses on a comprehensive literature review. Reviews on the pavement structure design, weak soil stabilization method, types of stabilizers, stabilization mechanisms and the main strength indications have been given.

Chapter 3 describes the characteristics of the experimental materials (soils, stabilizers) and the methodology used in this study.

Chapter 4 discusses the effect of different stabilizers on the mechanical properties of the stabilized soil.

Chapter 5 presents the effect of sampling method and curing condition on the mechanical properties of the stabilized soil.

Chapter 6 demonstrates the effect of wetting-drying cycles on the unconfined compressive strength of the stabilized soil.

Chapter 7 provides numerical simulation results for a pavement using the stabilized soil as the embankment materials in reality.

Chapter 8 summarizes the major findings of this research and provides suggestions for the future work

Chapter 2: Literature review

2.1 Pavement and subgrade structure

Pavement structure, composed of a surface course, a base course and a subbase course, generally lies on the top of the subgrade (Figure 2.1). Surface course is the top layer of the pavement structure which directly exposed to traffic loads. Hence, the surface course is usually built by materials with high qualities, such as asphalt or cement, to prevent an excessive rutting on the pavement surface. Base course normally uses crushed rock or cementitous materials. It works as a good support to distribute the stresses from the upper layers to the underlaying layers. The sub-base works as a conjunction between the base course and the subgrade. It can help to resist flexure in the base course. The subgrade layer comprises a roadbed layer and an embankment (including upper and lower embankment). The materials selected for the roadbed are carefully compacted to provide uniform support to the pavement structures. The roadbed and embankment layers are usually filled with granular materials. The types of the granular materials used as the fills are strictly restricted. According to the specification for the design of highway subgrades in China (China Specifications, 2015), there are several requirements for soil materials used as subgrade fills. First, sand and gravels are suggested for the subgrade, and the maximum particle size should be less than 100mm and 150mm for roadbed and embankment fills, respectively. The second requirement is for the CBR as given in Table 2.1. The third requirement is the degree of compaction. Finally, the resilient modulus of pavement subgrade surface should meet the requirement in the standard (China Specifications, 2015). For embankment fills, it also requires that the liquid limit and plastic index should be no larger than 50% and 26, respectively. Also, soaking embankment, bridge and culvert abutment and wall back of retaining wall should be filled by the materials with a good permeability. Fine grained soil stabilized by inorganic binders can be used as an alternative choice for the embankment.

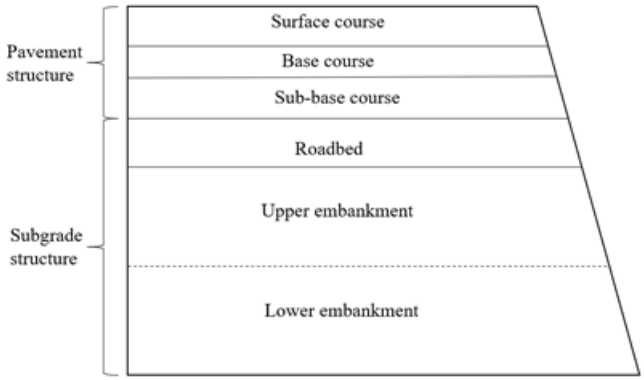

Figure 2.1 Typical structure of a flexible pavement structure and its subgrade

Table 2.1 Minimum requirements of CBR for subgrade fill

Embankment section		Depth below pavement structure (m)	Minimum CBR requirement (%)		
			Expressway, grade I highway	Grade II highway	Grade III and IV highway
Upper roadbed		0~0.3	8	6	3
Lower roadbed	Light, medium and heavy traffic	0.3~0.8	5	4	3
	Extra heavy traffic	0.3~1.2	5	4	-
Upper embankment	Light, medium and heavy traffic	0.8-1.5	4	3	3
	Extra heavy traffic	1.2-1.9	4	3	-
Lower embankment	Light, medium and heavy traffic	Lower than 1.5	3	2	2
	Extra heavy traffic	Lower than 1.9			

The side slopes of embankment should be designed according to the mechanical properties of filling materials, the height of the side slope and the in-situ engineering geological conditions. Table 2 shows the suggested maximum slops for the embankments designed with different heights.

Table 2.2 Maximum slope ratio for embankment side slope

Type of soil fill	Slope	
	Upper height (⩽8m)	Lower height (⩽12m)
Fine grained soil	1: 1.5	1: 1.75
Coarse grained soil	1: 1.5	1: 1.75

Giant grained soil	1: 1.3	1: 1.5

2.2 Weak soil stabilization method

In order to effectively treat and convert the slurry and dredged weak soil into renewable resources, extensive and in-depth researches on the dewatering treatment and comprehensive utilization of slurry and weak soils have been studied by many researchers. There are many stabilization methods such as physical method, chemical method and so on. Details of these methods are given below.

2.2.1 Physical method

For the soils used as filling materials, physical methods such as dewatering and reclamation by pumping filling are generally used to improve the strength. The commonly applied methods for dewatering are air-curing drying, mechanical dewatering and bag filling dewatering, etc. Air-curing drying, as the name implies, the excess moisture in the dredged soil can be removed by air drying and evaporation until the soil strength meet the requirements for fill materials. However, this method is only suitable for the treatment of a small amount of soil and must have enough space for air exposure. Furthermore, this method also greatly affected by the weather. The dewatering efficiency is negatively affected on rainy days. Mechanical dewatering is one of the most common way for dewatering treatment. Centrifuge or filter press facility are used. Through mechanical dewatering, the moisture content of soil can be reduced to a level close to the liquid limit and the secondary treatment is required to gain more strength to meet the construction requirement. This method is more suitable for the soil with a large sand content and relatively low water content (Detzner et al., 1998). For the soils with a high sand content, bag filling dewatering would be a more suitable method by using high pressure bag filling and consolidation drainage. The bag filling dewatering method has the characteristics of fast construction speed, low cost and using local materials. it should be noted that this method is not suitable for the soil with a high clay content (Zhang, 2013).

Reclamation by the pumping filling method has become an ideal way for especially coastal countries and regions for the treatment. The first stage of this method is to build a

cofferdam in the area which needs to be filled, the second step is to fill the cofferdam with soil and reinforce the foundation after then. The main methods used for filling consolidation are surcharge preloading method, vacuum preloading method, vacuum surcharge combined preloading method, dynamic drainage consolidation method and so on. The basic idea of the above consolidation methods is drainage consolidation. By applying a certain load after the setting of the vertical drainage system, the pore water in the soil will be discharged. Hence, the pore ratio will be reduced, and the strength of the filling soil will increase gradually. The disadvantages of the pumping filling method are high cost, long construction period.

All these physical treatment methods have a common problem that they cannot solve the secondary pollution caused by the pollutants contained in the dredged soil. The secondary treatment needs to be carried out to reduce the harm caused by secondary pollution.

2.2.2 Chemical method

The chemical method normally refers to a stabilization treatment. It can strengthen the soil through the physical and chemical reactions of various stabilizers. The stabilized soil has been applied as the structural filling materials in pavement engineering. At present, the stabilizers applied for weak slurry are cement, lime and so on. The stabilization mechanisms of these stabilizers will be clarified in the subsection 2.3. With the remixing of stabilizers and soil, hydration reactions will happen between water and stabilizer. Water in the soil would transfer from free water to bound water. The bound water enhances the binding force between the soil particles to improve the strength of weak soil (Conner, 1990； Tang et al., 2001； Feng et al., 2001). The manufacture of chemical stabilizer is relatively mature. The weak soil is first transported to the stabilization working platform. Then the weak soil is fed into the pre-treatment hopper by unloading the soil grab to remove debris and stones in the soil and then injected the soil into the soil storage tank. After then, the soil in the soil storage tank is fed into the stabilization treatment machine to react with the stabilizers. After the chemical stabilization, the treated weak soil can be transported to the construction site by vehicles or other conveying tools after chemical stabilization. There have been a lot of engineering practice cases in chemical stabilization treatment (Zhang et al., 2004a).

2.2.3 Heat treatment method

Another treatment method is the heat treatment with a high temperature environment. The heat treatment method is to treat the weak soils in the ways of sintering or melting under a high temperature. The purposes of sintering treatment is to make the separation between water and soil, the organic components decompose, bond building between soil particles and the melting of inorganic matter through high temperature treatment. And finally going through the process of cooling, so that the soil fusion would produce the stabilized particles with a certain strength (Dalton et al., 2004). The stabilized soil obtained from sintering treatment is mainly used for bricks and tiles burning (Yin and Gong, 2011). The melting treatment is to heat the soil to a temperature of 1200 to 1500℃. The melting treatment can melt the organic contaminant and increase the inorganic contaminants' inert.

From the analyses above, it can be known that the physical methods have the disadvantages of time consuming and secondary pollution. Heat treatment method has disadvantages such as high energy consumption and harsh treatment conditions. Hence, although there are three treatment methods, chemical stabilization is the most ideal method which has the characteristics of flexible, wide application, low cost, environmentally friendly and simple construction technology. Chemical stabilization is an ideal method for the treatment of a large amount of dredged soil.

2.3 Stabilizer

2.3.1 Types of stabilizers

There are many types of soil stabilizers. They can be divided into liquid and solid stabilizers based on their appearance forms. Based on the main component, they can be divided into inorganic stabilizer, organic stabilizer, biological enzymes, composite stabilizers and so on (Guo, 2007; Bai, 2014). The inorganic stabilizers are composed of a variety of excitants combined with the main stabilizer, such as the industrial wastes. This kind of stabilizers are generally powdery, such as cement, lime and fly ash. The advantages of these stabilizers are low cost and good long-term strength. The defects are large usage, high transportation cost and

low early strength to meet the construction requirement. Organic stabilizers, such as sodium silicate, ethoxy line resin and high polymer material can react with soil particle through an ion exchanging process to form the stabilized soil structure. This type of stabilizer can improve both early and long-term strength of the weak soils with a small amount. It is convenient and controllable in practical construction. However, the stabilization efficiency would be affected by environmental factors compared with the inorganic stabilizers, the service life of the soil stabilized by organic stabilizers is short. Biological enzymes come from the fermentation of organic matters, the appearance forms of them are normally liquid. Based on the catalytic actions of biological enzymes, the adhesiveness of soil particles has been improved to form a firm impermeable structure. Soil stabilized by biological enzymes stabilizer has a short service life and relatively low water stability. But it is nontoxic, would not lead to environment disruption and soil pollution. Composite stabilizers are combined by two or more types of chemicals to form new materials. To meet the specific requirements in different projects, the combinations can be varied according to the main stabilizers or activators.

2.3.2 Stabilization mechanisms

Different kinds of stabilizers have different stabilization mechanisms. It is necessary to understand the stabilization mechanisms of different stabilizers. This thesis has reviewed the stabilization effects of cement, lime, fly ash and gypsum as a single or part of the combined stabilizers in soil. The stabilization mechanisms of them have been summarized below.

2.3.2.1 Stabilization mechanisms of cement

The most common-used stabilizer is cement, for which the stabilization mechanisms have been clarified by many researches previously (Bell, 1995； Prusinski and Bhattacharja, 1999). The cement mineral and the water in the soil undergo violet hydrolysis and hydration reactions after the cement is mixed with soil. At the same time, calcium hydroxide ($Ca(OH)_2$) is decomposed from the solution and other hydrates would form. The reaction procedures have been shown below:

(1) The hydration reaction of tricalcium silicate ($3CaO \cdot SiO_2$) can form calcium silicate hydrate (CSH) gel and calcium hydroxide, this reaction is the decisive factor of the strength of stabilized soil:

$$2(3CaO \cdot SiO_2) + 6H_2O \text{ —— } 3CaO \cdot 2SiO_2 \cdot 3H_2O + 3Ca(OH)_2$$

(2) The hydration reaction of dicalcium silicate ($2CaO \cdot SiO_2$) can form CSH gel and calcium hydroxide, this reaction is resource of the long-term strength of stabilized soil:

$$2(2CaO \cdot SiO_2) + 4H_2O \text{ —— } 3CaO \cdot 2SiO_2 \cdot 3H_2O + Ca(OH)_2$$

(3) The hydration reaction of tricalcium aluminate ($3CaO \cdot Al_2O_3$) can form calcium aluminate hydrate (CAH) gel. This reaction has the fastest hydration velocity to promote early setting of cemented soil:

$$3CaO \cdot Al_2O_3 + 6H_2O \text{ —— } 3CaO \cdot Al_2O_3 \cdot 6H_2O$$

(4) The hydration reaction of tetra-calcium aluminoferrite ($4CaO \cdot Al_2O_3 \cdot Fe_2O_3$) can form CAH and calcium ferrite hydrate gels to improve the early strength of cement stabilized soil:

$$4CaO \cdot Al_2O_3 \cdot Fe_2O_3 + 2Ca(OH)_2 + 10H_2O \text{ —— } 3CaO \cdot Al_2O_3 \cdot 6H_2O + 2CaO \cdot Fe_2O_3 \cdot 6H_2O$$

(5) The reaction of calcium sulfate (CaSO4), tricalcium aluminate and water can produce ettringite ($3CaO \cdot Al_2O_3 \cdot 3CaSO_4 \cdot 32H_2O$, also called cement bacillus). A large amount of free water would be fixed as crystal water during this procedure:

$$3CaSO_4 + 3CaO \cdot Al_2O_3 + 32H_2O \text{ —— } 3CaO \cdot Al_2O_3 \cdot 3CaSO_4 \cdot 32H_2O$$

When various hydration products of cement have been formed, some of them continue to harden to form a cement stone skeleton structure, while others interact with soil. The forms of these interaction can be summarized as below:

(1) Ion exchange and agglomeration. After hydration of cement, $Ca(OH)_2$ coexists with Ca^{2+} and OH^- in the gel. The minerals that make up the clay are plate-like or needle-like crystals which synthesized with SiO_2 as a skeleton, usually with Na^+ and K^+ ions in its surface. The precipitated Ca^{2+} would carry out adsorption exchange with the Na^+ and K^+ ions in the soil. As a result, a large number of soil particles form large soil aggregates. Because of the strong adsorption activity of the cement hydration product $Ca(OH)_2$, these large soil aggregates would be further combined to form a chain structure of cement, which closes the pore between the soil aggregates and forms a stable connection.

(2) Pozzolanic reaction (also called hard coagulation reaction). With the deepening of the hydration reaction of cement, a large amount of Ca^{2+} is precipitated in the solution. When the amount of Ca^{2+} ion exceed the requirement of ion exchange mentioned above, a chemical reaction occurs with a part of SiO_2 and Al_2O_3 from clay minerals in alkaline environment to form stable crystalline minerals $CaO\text{-}Al_2O_3\text{-}H_2O$ series of aluminite lime hydrates and $CaO\text{-}SiO_2\text{-}H_2O$ series of silicate lime hydrates which are insoluble in water.

(3) Carbonation. The free $Ca(OH)_2$ in cement hydrates continuously absorbs the CO_2 in water and air to form $CaCO_3$, which improve the strength of the soil. Cement stabilized soil is the result of the combination of the skeleton action of cement stone and the physical and chemical actions of $Ca(OH)_2$. The latter actions make clay particles and micro clusters form a stable aggregate structure, while the cement stone encapsulates these aggregates and connects them into a strong whole.

The cement stabilized soil is limited by the soil type. The effects of strengthening clay, organic soil and saline soil with high plastic index are not good. Both the dry shrinkage

coefficient and temperature shrinkage coefficient of cement stabilized soil are large than acceptable if excessive cement is added. And the cement stabilized soil is normally easy to crack with too much cement addition (Natt and Joshi, 1984； Hausmann, 1990). The initial and final setting time of cement is quite short. Hence, it is generally required to complete each process from adding water and soil mixing to the end of the rolling no longer than 3 to 4 hours.

2.3.2.2 Stabilization mechanisms of lime

Lime is also widely used in the practice to stabilize weak soils, but the primary stabilization mechanisms of lime are different from cement. A series of chemical and physicochemical reactions occur between lime and soil after lime is added to the soil. The main reactions include the ion exchange reaction, the crystallization reaction of $Ca(OH)_2$, the carbonation reaction and the pozzolanic reaction. The dominant component of lime is CaO. When lime is added into the soil, it reacts with water to form $Ca(OH)_2$. And $Ca(OH)_2$ dissociates into Ca^{2+} and OH^- ions with the participation of water. The ion exchange reaction of Ca^{2+} can occur with Na^+ and K^+ ions, so that the adsorption layer of colloid would be thinned, and the potential would be reduced. Hence, the clay colloid would be flocculated, and the wet slump of the soil has been improved. As a result, the initial water stability of the lime stabilized soil has been obtained (Sherwood, 1993； Bell, 1996). The crystallization reaction of $Ca(OH)_2$ makes lime absorb water to form water-bearing crystal lattice ($Ca(OH)_2 \cdot nH_2O$). The formed crystals combine with each other, and they would combine with soil particles to form cocrystals. The soil particles would be glued as a whole combination, so that the water stability of lime stabilized soil would be improved. The carbonation reaction of $Ca(OH)_2$ is the chemical reaction between $Ca(OH)_2$ and CO_2 in the air and water to form $CaCO_3$. The product has a relatively high strength and water stability. The formation of $CaCO_3$ would cause the cementation of soil particles to strengthen the stabilized soil. The pozzolanic reaction is the dissociation of active silicon and aluminum minerals in the soil under the alkaline excitation of lime. With the participation of water, the products of dissociation would react with Ca(OH)2 to form water-bearing cementations such as calcium silicate and calcium aluminate. These cementations would transform from the gel state to the crystal state gradually within a long time. The

transformation would make the stiffness of lime stabilized soil increase, and the strength and water stability would be improved.

According to Hilt and Davidson (1960), when the lime content is within 1% to 3%, all the strength came from ion exchange reaction. with an increasing lime content, the excess ions cannot be effectively adsorbed and fixed by the clay minerals. Even though pozzolanic reactions can further happen between the remnant calcium hydroxide and active clay minerals to enhance the strength, the reaction rate is relatively slow (Petry and Little, 2002).

The strength of soil stabilized by lime develops slowly, which affects the progress of construction. At the same time, lime stabilization has an optimum content to improve the soil. When the lime content excesses the optimum content, the strength of the lime stabilized soil would reduce instead. And the water stability of the lime stabilized soil is quite poor. For some projects with high stabilization strength requirements, lime cannot meet its requirements of strength and stability.

2.3.2.3 Stabilization mechanisms of fly ash

Fly ash, as a waste binder, is also used for soil stabilizations due to its cost-effectiveness and environmental friendliness. Fly ash is a kind of industrial waste slag which is mainly composed of microbeads and porous glass after the coal powder is burned in the power plant boiler in a suspended state. Normally, fly ash is produced by blowing pulverized coal into a coal boiler at high speed with hot air. The main chemical components of fly ash are SiO_2, $Al2O_3$, MgO, Fe_2O_3 and CaO. The fly ash has a CaO content between 1% to 10%, called ordinary fly ash , also called low calcium fly ash (LFA), this kind of fly ash is the mainly used type in China. If the CaO content is more than 10%, this type of fly ash is called high calcium fly ash (HFA). The microstructure of fly ash is composed of glass phase and crystalline phase. Most of the ordinary fly ash contains crystalline minerals. And the main minerals in the crystalline phase are quartz, magnetite, mullite and so on. The minerals of these crystalline phases are inactive at room temperature, thus reducing the activity of ordinary fly ash.

To active the activity of ordinary fly ash, chemical activation is the main method applied in practice. The chemical activation of fly ash mainly activates the activity of fly ash through

alkaline excitant. Because of the addition of alkaline excitant, the concentration of OH^- in the solution increases. When the fly ash is added into the alkaline solution, some of the silicon-oxygen bonds (—Si-O—) and aluminum-oxygen bonds (—Al-O—) in the active glass phase break. These broken bonds become unsaturated active bonds. Thus, the aluminosilicate structure in the glass body disintegrated to form an irregular network structure similar to the glass body (Tong, 2015).

The effect of fly ash on improving soil properties mainly comes from the hydration and hardening of fly ash. If the increase in the strength of the fly ash stabilized soil is only derived from the hydration of the fly ash, the soil is regarded as a component with stable chemical properties. The fly ash particles would cement the surrounding clay particles during hydration to form a hard skeleton with a continuity which would enclose the soil particles without any variation. This hard skeleton would fill the pores and decrease the permeability and swell-shrink characteristic of the soil, increase the water stability of the stabilized soil. This is the first type of stabilization reaction. If the stabilized soil is clay, in addition to the hydration and hardening process of fly ash, the hydration products of fly ash would react with the clay to produce more stabilization products and strengthen the connection between soil particles and between soil particles and fly ash particles. This is the second type of stabilization reaction. The second type of stabilization reaction would reduce the plasticity and water expansion of the clay composition itself (Bai, 2009).

However, it was found that the addition of fly ash alone as the stabilizer for soils cannot promote the strength effectively (DiGioia and Nuzzo, 1972； Sivapullaiah and Jha, 2014； Christopher et al., 2006). According to previous reviews, an alkaline environment is necessary to improve the activity of fly ash and accelerate the hydration process remarkably. According to the dissolving experiment done by Fraay et al. (1989), with a pH value larger than 13.4, the glass body structure of fly ash would be destroyed. Based on these reactions, more cementious gels and more strengths can be obtained (Taştan, 2005). Considering that the hydroxide ion content in fly ash is limited, lime or other excitation agents are always used as supplements (Kumar et al., 2007； Chen et al., 2013). Comparing with cement, the reaction rate of fly ash is quite slow and the strength is highly dependent on the curing age, but the swelling and

shrinkage of stabilized soils can be effectively reduced (Little and Nair, 2009； Cokca, 2001).

2.3.2.4 Stabilization mechanisms of gypsum

Gypsum, as the main source of sulfate, can enhance the strength of soil with rich calcium aluminate by forming niddle-shape ettringites. The ettringite produced by the pozzolanic reaction is an expansionary hydrate product. The ettringite would fill in the void of soil structure, therefore gypsum has been commonly used as stabilizers or a supplement for soil stabilization (Jin et al., 2014). However, more gypsum does not lead to a larger strength of stabilized soil. The addition of gypsum exists an optimum content to maximize the strength behavior of gypsum stabilized soil. Huang et al. (2007) stated that the excessive addition of gypsum would produce too much ettringite. The expansion of ettringite would destroy the formed structure and lead to the decreasing of strength. In addition, the optimum content of gypsum also depends on the type of stabilized soil. For different types of soil, they have different distributions and amounts of structure voids. The structure voids decide the effects of strength improvement by ettringite. And different types of soils have different pH values. The alkaline environment is quite important for gypsum stabilization. The concentration of OH^- decides the performance and expansion character of ettringite. It is the decisive factor for gypsum stabilization of soil (Huang and Hu, 1998).

2.3.3 Stabilizer combinations

According to the previous analyses of stabilization mechanisms for four types of stabilizers, it could be found that the environmental requirements and stabilization processes of these stabilizers have similarities in some aspects. They could be considered as supplements for each other. Therefore, in order to take better advantage of any single stabilizer, a combination of them is always used in the practice (Parsons and Milburn, 2003). For instance, the cement is always applied along with lime to facilitate its pozzolanic reaction (Åhnberg and Holm, 2009； Jauberthie et al., 2010； Ouhadi et al., 2014). Some researchers also replaced a portion of the cement with fly ash so that the required strength and a better shrinkage and swelling resistance property can be achieved (Indraratna et al., 1995； Wang and Xu, 2012). Besides, a remixing

stabilizer containing cement and fly ash is also commonly used in practical construction. the cement works as a main stabilizer as well as the alkali activator for the fly ash (Wang and Xu, 2013； Kogbara et al., 2013). Moreover, adding a proper portion of gypsum as an additive into the remixing stabilizer can further increase the strength, as the expansion of the generating ettringites can fill the voids in the stabilized soil structure (Jin et al., 2014). However, there exists an optimum content of gypsum which is similar to the stabilization of gypsum itself. The excessive expansions of ettringites may destroy the whole structure of the stabilized soil on a micro level and thereby resulting in a reduction in the strength (Jin et al., 2014； Huang et al., 2007). Another possible reason is that the reaction process of gypsum is slow in the stabilized soil. If excess gypsum is added, the unreacted gypsum may weaken the bonds between soil particles and the cementitious compounds due to their platy shapes (Kumar et al., 2007； Kolay and Pui, 2010). Currently, the selection of the components for a remixing stabilizer is mostly based on the understanding of their reaction mechanisms; however, the effectiveness of each component on the properties of the stabilized soil is not clear, which makes the selection of an optimal formula for the remixing stabilizer lack a basis.

2.4 Strength indicators

2.4.1 Unconfined compressive strength

Unconfined compressive strength is one of the basic strength indicators of the stabilized soil. Unconfined compressive strength is the ultimate resist strength of soil sample under an axial load when the confining pressure is zero. The unconfined compression tests have been conducted in many researches to investigate the engineering performance of treated soil. Gao et al. (2014) studied the unconfined compressive strength of loess. They selected the loess as experimental material to investigate the influence of density and moisture content on the unconfined compressive strength of loess sample. And they analyzed the variation of elastic modulus of loess sample with moisture content and the dry density. This study aims to provide theoretical and experimental basis for the construction of loess as fill. Xu (2015) also conducted the research to study the effect of many influence factors, such as the cement content, curing time, curing environment and moisture content on the unconfined compressive strength

of the cement stabilized soils. Chen et al. (2011) studied the unconfined compressive strength of lime stabilized expansive soil. The effect of curing times were investigated and the results show that there exists an optimum lime content to maximize the compressive strength. And the unconfined compressive strength and the curing age shows a linear relationship at the early curing stage.

2.4.2 California Bearing Ratio

California Bearing Ratio (CBR) is a strength obtained from CBR tests. The CBR test is a penetration test used to evaluate the subgrade strength of roads and pavement layers. CBR test was developed by the California Division of Highways to classify and evaluate the soil-sub grade course and base coarse material properties for flexible pavements. During the test, the materials would be penetrated at a standard rate of 1.25 mm/min with a standard piston with a diameter of 50 mm. Test will be ended when the penetration depth reaches 2.5 mm and the CBR value can be calculated. This CBR value can guide pavement thickness combination design.

CBR test has been conducted in many projects. Purwanto et al. (2020) conducted the CBR test for a soft clay soil stabilized by a gypsum plafond waste. They stabilized the soft soil with different ratios of gypsum plafond waste and carried out the CBR tests both soaked and unsoaked. The unsoaked samples had higher CBR value than soaked samples' value. The highest CBR value for the soaked cases was 6.25 with a gypsum plafond waste mixture of 11.44%, and the highest CBR value for the unsoaked cases was 6.85 with a gypsum plafond waste mixture of 15.75%. Chegenizadeh and Nikraz (2011) investigated the effect of fiber inclusion on CBR value. The geosynthetic fiber is one type of geomaterials used widely in civil engineering applications such as pavement embankment systems. They conducted a series of CBR tests for unreinforced samples as well as the reinforced samples with different fiber contents (i.e. 0.1%, 0.3%) and considered the effect of different fiber lengths (i.e. 10 mm, 25 mm and 50 mm). The results indicated that both the increments of fiber contents and fiber lengths would lead to an increase of the CBR value. Therefore, the short randomly distributed fiber is an effective material to improve the engineering performance of pavement layers in

practical projects. Smith and Pratt (1983) conducted in situ CBR tests and compared the laboratory results. The results show that the in situ CBR values were generally lower than the laboratory values.

2.4.3 Triaxial shear strength

Shear strength of soil is mainly characterized by cohesion and internal friction angels. These parameters can be obtained through triaxial shear tests. To simulate different in-situ conditions, triaxial shear tests can be classified as: unconsolidated undrained test, consolidated undrained test and consolidated drained test. Each group of test needs to be completed under different cell pressure to obtain the failure line for the Mohr-Coulomb circles, thus the cohesion and friction angle of the material can be determined. Comparing with the direct shear test, change of the pore water pressure of soil samples can be measured accurately in triaxial tests, therefore the change of effective stress in soil can be obtained quantitatively (Zhou and Shen, 2013).

Triaxial shear tests have been carried out in many previous studies. Hamidi and Hooresfand (2013) investigated the effect of fiber reinforcement on triaxial shear behavior of cement stabilized sand soil considering confining pressures of 100, 300 and 500 kPa. The results indicated that the fiber reinforcement can improve the peak and residual shear strengths of cement stabilized soil and change its brittle behavior to a more ductile state. Shi et al. (2011) studied the triaxial shear strength characteristics of lime stabilized soil reinforced with the inclusion of polypropylene fiber. In this study, soil samples stabilized with different lime ratios (10%, 20% and 30%) have been reinforced with different fiber ratios (0.05%, 0.15% and 0.25%). The results showed that the fiber reinforced lime soil samples had higher peak residual stress and shear strength compare to normal lime soil samples without fiber reinforcement. In addition to soil samples with stabilization or fiber reinforcement methods, Matalucci et al. (1970) selected Vicksburg loess as the soil material for triaxial shear test. The aim of this study is to investigate the influence of microstructure of the loess on the triaxial shear strength and the relationship between natural fabric anisotropies of the loess and the orientation of applied stress distribution. They conducted two series of triaxial shear tests. The results illustrated that when the direction of principal stress was perpendicular to the grain orientation, the loess

samples would have the maximum ultimate strength. And the ultimate strength would decrease when the principal stress was 45° to the fabric plane. Furthermore, the slope of the Mohr-Coulomb fracture line increased at higher confining pressure indicated that poorly cemented sand, sandstone, silt or siltstone may undergo two failure modes. One of the modes is cement bonds are disrupted at small strains and the other one is the excessive internal shearing resistance of granular components at larger strains.

2.4.4 Splitting tensile strength

Splitting tensile strength (or called 'indirect tensile strength') of pavement materials is a considerable parameter for pavement design. Sufficient tensile strength can prevent pavement from cracking. Splitting tensile strength tests have been applied to measure the tensile strength of soil samples indirectly. The splitting tensile strength test is to load the cylinder samples for a transverse tension stress. The stress is distributed and applied by two parallel plates in two diametrically opposite points on the diameter of the cylinder surface which leads to propagation of cracks through the paste. The splitting of sample along the vertical plane would happen because of the high tensile stresses (Jaber et al., 2018).

The influencing factors of soil splitting tensile strength have been studied in many projects. Liu and Wang (2019) conducted the splitting tensile strength test for cement stabilized laterite granules. They thought the strength of cement stabilized materials is not only determined by the material properties, but also change with the size, load and boundary conditions of the samples. They prepared the test samples with a ratio of diameter to height of 1:1 or 1:2. The cement content is 2.5%, 3%, 4% or 6% and the curing age is 90 days, 180 days or 360 days. According to the experimental results and SPSS (Statistical Product and Service Solutions) analysis, the following conclusions had been obtained. With the increase of cement content, the splitting tensile strength of cement stabilized laterite granules would increase linearly. With the increasing of curing age, the splitting tensile strength increases rapidly at early stage, while the grow rate slows down latterly. Finally, the strength became stable. In addition, with a smaller ratio of diameter to height, the different compaction stages of the sample would be more obvious. The vertical deformation failure became larger, while the peak

stress at failure became smaller. In addition, it has been found that the temperature gradient formed between the interior of sample and the external environment is more obvious. All these variations would result in a decreasing splitting tensile strength. Jiang et al. (2019) investigated the splitting tensile strength of cement stabilized soil which also be reinforced by glass fiber. The influencing factors in this study were fiber content, fiber length, cement content and curing age. The splitting tensile strength of soil samples increased with the increment of fiber content and reached a peak strength value when the fiber content was 0.2%, then the strength began to decrease. However, the peak strain of the samples always increased with the increase of fiber content. For the fiber length, the grow trend of strength was similar to the fiber content part. The peak value appeared when the fiber length was 6 mm. In addition, with the increasing of curing ages, the splitting tensile strength increased, but the peak strains decreased.

2.5 Main influence factors on the strength of stabilized soil

2.5.1 Moisture content

Moisture content is one of the most important characteristics of soil. Water acts as a dominant component which exerts controlling influence on most of the physical, chemical and biological processes. The water in the soil works as both a lubricant and a binder among the soil particles, thereby affecting the structural stability and strength behavior of soil (Topp and Ferre, 2002). Bláhová et al. (2013) conducted direct shear tests and stability analysis for clayey soil with an optimum content of 12%. They prepared the samples with the moisture contents on the dry side of the optimum moisture content at 9%, 10% and 11%. Because the samples with moisture contents below 9% and above 12% were not possible to be prepared without destroying the original structure of the soil specimen. The experimental results showed that shear strength parameters were significantly affected by the moisture content of soil samples. With the increasing of moisture content, the overall shear strength would decrease. They stated that with the moisture content on the dry side of the optimum, the soil structure tends to be more flocculated which leads to the improvement of shear strength. while on the wet side of the optimum, the soil structure would be more dispersive. This conclusion also be summarized by Lambe and Whitman (1991) that the particles of flocculated soil would have higher strengths

than the same type of particles which in the soil at the same void ratio but in a dispersed state. Liang et al. (2013) also investigated the influence of moisture content on the shear strength of treated clayey soils. They conducted the triaxial shear test for clayey soil remixing with steel slag, and the moisture contents of the test samples were varied from 15% to 22%. The experiment results demonstrate that, with the increase of moisture content, the cohesion increases, while the internal friction angel decreases. In addition, the maximum stress difference increases at first and then decreases. When the moisture content is 18% which is close to the optimum moisture content, the largest value of maximum stress difference can be obtained.

In addition to the shear strength, Muntohar (2005) conducted the unconfined compression test to investigate the influence of moisture content on the unconfined compressive strength of stabilized soil with lime and rich husk ash. The samples with moisture contents on both dry and wet side of the optimum moisture content had been prepared. The unconfined compression test results indicated that the unconfined compressive strength of the stabilized soil samples decreases with the increase in molding moisture content, but it is still larger than un-stabilized soil samples. And the strength would reach the peak value when the moisture content is close to the optimum moisture content. Because the soil samples would have the maximum dry density at the optimum moisture content. Senol et al. (2002) also elaborated these conclusions.

2.5.2 Wetting-drying (W-D) cycle

In pavement engineering field, variations in climatic conditions have already been recognized as an important aspect which can affect the mechanical performance of pavement. (Chen et al., 2005； Ahmed and El Naggar, 2018； Sobhan et al., 2016). Experimental tests considering wetting-drying cycles can simulate the variation of climatic conditions and guide practical construction.

In different projects, the W-D cycles were set up with different conditions. The differences mainly reflected in the number of the W-D cycles and the procedures and environment for each W-D cycle. The variation of cycle procedure and environment might cause different reactions inside the soil samples, therefore affect the long-term performance of stabilized soil

samples. Khoury and Zaman (2002) investigated the effect of wetting-drying cycle numbers on the mechanical properties of aggregates stabilized by Class C fly ash. The resilient modulus, unconfined compressive strength and elastic modulus were all studied. For every W-D cycle, the specimen were placed in an oven at a temperature of 71℃ for 24 hours and then submerged it in water tank for 24 hours at room temperature. W-D cycles were applied on stabilized samples after they have been cured for 3 day or 28 days. And the numbers of W-D cycle in this research were set up as 4, 12 and 30 times. According to the experiment results, they found that the resilient modulus of stabilized samples with 28 days' curing age reached the peak value with 12 W-D cycles. With the further increase of W-D cycle number, the resilient modulus started to decrease and reached a lower value compared with the samples which subjected to no W-D cycles. For 3 days' cured samples, the resilient modulus value increased by 55% due to the application of 30 W-D cycles. Furthermore, samples with 28 day's curing age were more vulnerable to a good deal of reduction in resilient modulus values than the samples with 3 days' curing age. Effect of curing ages on UCSs and elastic moduli also exhibited similar trends to those of the resilient moduli. The values of UCS and elastic modulus increased with the increasing of W-D cycle numbers. And the increasing percentage was more significant during the early cycle period than long-term cycle with high cycle numbers.

Cheng et al. (2014) also studied the effects of W-D cycle numbers on the mechanical properties of loess solidified by SH stabilizer. Unconfined compression test and direct shear tests were conducted. For unconfined compression tests, the sample is submerged in water for 12 hours and then air dried for 12 hours for each W-D cycle. The W-D cycle numbers were 0, 5, 10 and 15. For direct shear test, the wetting and drying time were both extended to 24 hours. The numbers of W-D cycles were 0, 1, 2, 3, 4, 5, 10 and 15. Results show that the increasing W-D cycle numbers leads to an exponential decay of the unconfined compressive strength. For direct shear tests, the direct shear strength decreased dramatically after the early 3 to 4 W-D cycles, and both the cohesion and the internal friction angle decreased. With a further increase of the W-D cycles, the decreasing cohesion and internal friction angle became stable.

Cheng et al. (2017) used Yunnan laterite (which is one type of silty laterite with low liquid limit) as research subject to investigate the influence of W-D cycle number on the shear

characteristic. Undrained triaxial test has been performed on saturated laterite samples. They set the original moisture content of compacted sample as A, and then dried the sample to a moisture content B in an oven of 40℃. The dried samples were sealed and placed at room temperature for 24 hours. This purpose of this step is to make the moisture contents and temperature inside and outside of the samples reach an unanimity. The next step is to increase the moisture content to C by spraying water. After the wetting process, the samples were sealed and placed at room temperature for 24 hours. Finally, the moisture content of sample was decreased to the original value A using the same drying method descripted in the first step. The whole process was termed as one W-D cycle in their study. The experiment results show that the increase of W-D cycle number leads to a significant strain softening phenomenon, and all the peak shear strength, peak shear strain, cohesion and internal friction angel would decrease. They thought the variation of shear characteristics were caused by the physical interaction between the laterite and the water and therefore the wetting and drying procedures lead to a decreasing shear strength. When the sample is under a drying condition, the internal moisture content is higher than the external moisture content, so the water would move toward the surface of sample. The decreasing moisture content enhances the adsorption capacity between soil particles and decreases the particle spacing. As a result, the shrinkage crack would generate easily, which makes the water enter the soil more easily. Besides, the increase of particle spacing causes an expansion of soil sample therefore some expansion cracks. When continuous W-D cycles are applied, the shrinkage and expansion of soil sample continuously repeated, which could result in more and more cracks.

Wang et al. (2017) used fiber-reinforced stabilized sand as experimental material for W-D cycle test. In this project, curing age of stabilized sand samples were 3, 7 or 14 days. For each W-D cycle, the samples were placed in the oven at a temperature of 70℃ for 12 hours drying, and then submerged into a water tank at a constant temperature of 22±1℃ for 12 hours. The unconfined compression test results show that the increase of W-D cycle number would lead to a significant decrease of unconfined compressive strength. The first 6 W-D cycles significantly decrease the unconfined compressive strength by 43%. Then the decreasing rate gradually slows down for further W-D cycles. After 12 W-D cycles, the

unconfined compressive strength of samples decreased by 57%. In a micro-level, SEM and EDS tests were conducted. The microstructure SEM images after 6 W-D cycles obviously show that the spacings of needle-like network structure becomes larger when compared with those in the samples without W-D cycles. Because of the absorption and loss of water alternate continuously inside the samples some of the stabilizer components would loss with the loss of water. Cracks of framework structure formed by hydration products would appear and expand. At the end, the loss of stabilizer components and structure cracks would lead to a decreasing unconfined compressive strength. EDS test was applied for cement stabilized samples experienced 6 W-D cycles. The results indicate that after the W-D cycles, cement hydrates were precipitated in the form of crystalline salts of calcium and magnesium ions, and calcium has a large proportion in the salting out body. The above analysis showed that the hydrates of the original stabilizer components precipitate with water loss after the sample experienced W-D cycles, which leads to the destruction of the original hydrates network-like interconnected structure, and makes the pores of the hydrates connected structure become larger, which further weakens the strength of the soil samples. The strength of soil samples also decreased significantly after dry-wet cycle due to the transformation of the original solid needle-like network structure of the hydration products of some stabilizers into the more fragile salt-out junction crystal connection structure.

Chapter 3: Experimental materials and research methodology

3.1 Characteristics of soils

In this study, three types of soil have been selected for experiments. It should be noted that all the percentages (e.g. moisture content, stabilize content) in this study were calculated based on the weight of dry soil. Equation 3.1 shows the calculation example of moisture content.

$$Moisture\ content = \frac{the\ weight\ of\ water}{the\ weight\ of\ dry\ soil} \times 100\%$$

Equation 3.1 Calculation of moisture content

3.1.1 Fine grain soil

The first soil can be classified as CL according to the British standard BS5930: 2015 (BSI, 2015). This soil was taken from an expressway construction site in Ningbo, China. The location of the expressway construction site is shown in Figure 3.1. Figure 3.2 shows the gradation curve obtained by Bettersize 2000 Laser Particle Size Analyzer. According to the results of liquid-plastic limit combined determination test, the liquid limit, plastic limit and plastic index of the soil are 24.0%, 14.3% and 9.7%, respectively. Light compaction test was conducted on the fine soil according to the standard Proctor compaction test procedure in the British standard BS1377-2: 1990(BSI, 1990). The maximum dry density and the optimum moisture content of the fine CL soil obtained from the light compaction test are 1.81 x 10^3 kg/m^3 and 9.4% respectively. All these characteristics of fine CL soil were summarized in Table 3.1.

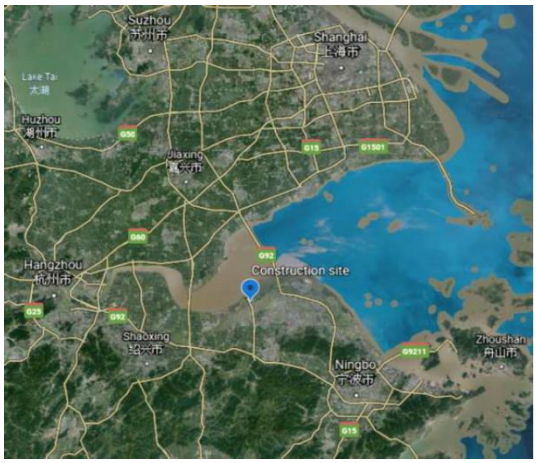

Figure 3.1 Location of the expressway construction site

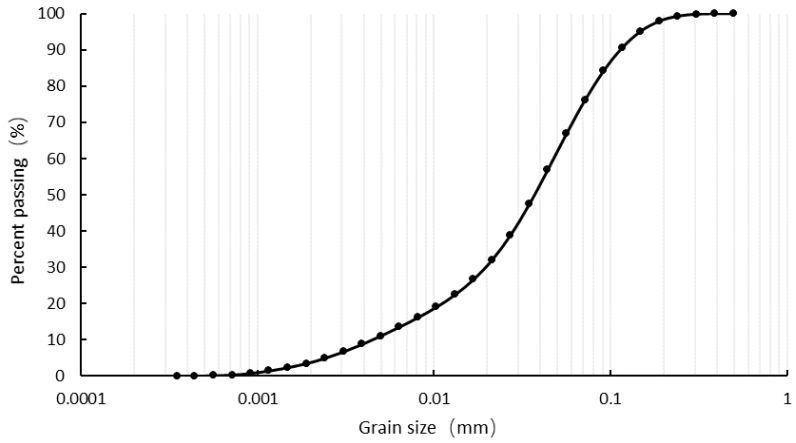

Figure 3.2 Gradation curve of the fine grain soil

Table 3.1 Physical characteristics of the fine grain soil

Liquid limit %	Plastic limit %	Plastic index	OMC %	Maximum dry density kg/m^3
24	14.3	9.7	9.4	1.81

3.1.2 Dewatered drilling slurry - A

Another soil is waste drilling slurry taken from the construction site in Ningbo, China. The slurry was pre-treated by a Plate and Frame Filter Press Dewatering System, forming soil cakes (dewatered soil) with a moisture content of around 26%. The physical characteristics of the soil cakes were given in Table 3.2. The main chemical components (Table 3.3) were determined by Epsilon 4 Benchtop X Ray Fluorescence (XRF) analyzer. The gradation curve

obtained by Bettersize 2000 Laser Particle Size Analyzer was plotted in Figure 3.3. According to the British standard BS1377:2-1990, 6.9%, 89.6% and 3.5% of the grains in mass are classified as clay, silt and sand particles, respectively.

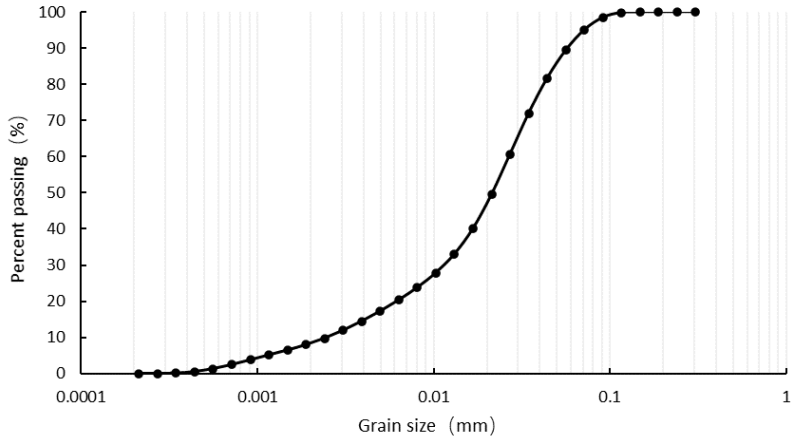

Figure 3.3 Gradation curve of the dewatered drilling slurry - A

Table 3.2 Physical characteristics of the dewatered drilling slurry - A

Liquid limit %	Plastic limit %	Plastic index	OMC %	Maximum dry density kg/m^3
29.7	19.6	10.1	19.5	1.72

Table 3.3 Chemical components of the dewatered drilling slurry - A

SiO_2	Al_2O_3	Fe_2O_3	CaO	K_2O	MgO	P_2O_5
73.02%	11.28%	4.29%	3.07%	2.65%	1.85%	0.54%

3.1.2 Dewatered drilling slurry – B

The dewatered drilling slurry – B was obtained from the same construction site as A. But they came from different excavation batches and the properties are different with A. Figure 3.4 shows the gradation of the dewatered soil – B. According to the standard, 5.1%, 84.2% and 10.7% of the grains are classified as clay, silt and sand particles, respectively. Table 3.4 shows the physical characteristics of the soil. And the chemical components of this soil are shown in Table 3.5.

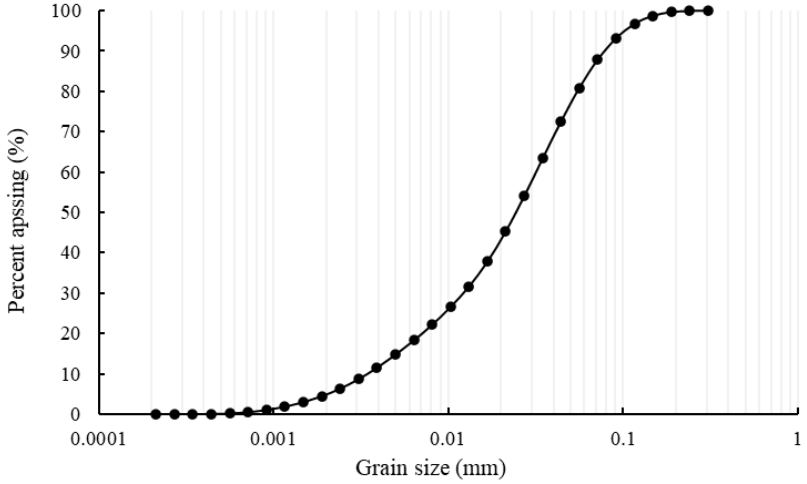

Figure 3.4 Gradation curve of the dewatered drilling slurry – B

Table 3.4 Physical characteristics of the dewatered drilling slurry - B

Liquid limit %	Plastic limit %	Plastic index
32.9	22.9	10.0

Table 3.5 Chemical components of the dewatered drilling slurry – B

SiO_2	Al_2O_3	Fe_2O_3	CaO	K_2O	MgO	Na_2O
65.53%	16.72%	5.66%	4.37%	3.07%	2.23%	1.34%

3.2 Stabilizers properties

The stabilizers used in this study are cement, lime, fly ash, gypsum and a commercial fluid stabilizer produced by a construction company in Ningbo, China.

3.2.1 Cement

The Portland cement CEM I 42.5 N used in this study was provided by Hailuo Cement Company, China. Figure 3.5 shows the appearance of the Portland cement.

Figure 3.5 Portland cement

3.2.2 Lime

The quick lime used in this study had a purity of larger than 98%.

3.2.3 Fly ash

The fly ash used in this study was classified as Class II, of which the chemical composition and the gradation are given in Table 3.6 and Figure 3.6. Figure 3.7 shows the appearance of fly ash.

Table 3.6 Chemical composition of the Class II fly ash

Components	Loss on ignition	SiO_2	Fe_2O_3	CaO	MgO	Al_2O_3
Mass percentage %	7.5	56.96	4.63	1.5	1.5	23.67

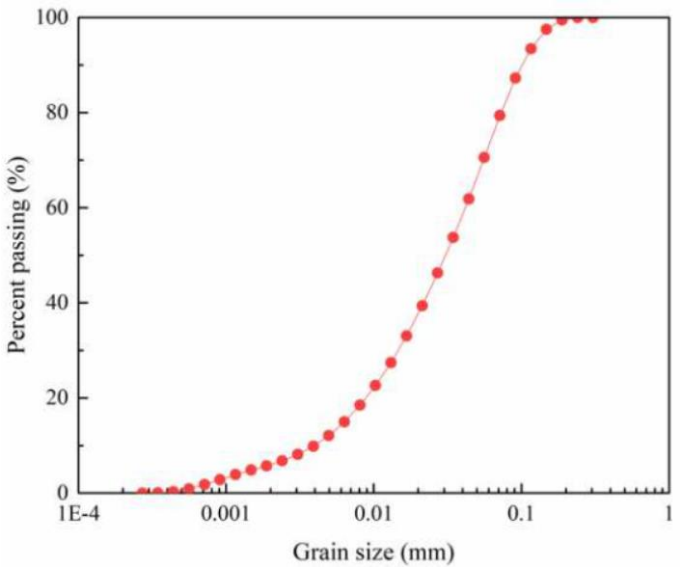

Figure 3.6 Gradation curve of the Class II fly ash

Figure 3.7 Fly ash

3.2.4 Gypsum

The gypsum used in this study was mainly composed of calcium sulphate dihydrate (≥ 99%).

3.2.5 Commercial stabilizer

The commercial stabilizer was provided by a construction company. It is a fluid stabilizer with a color of pale yellow. Figure 3.8 shows the appearance of the commercial stabilizer. The details of the commercial stabilizer had not been provided by the construction company.

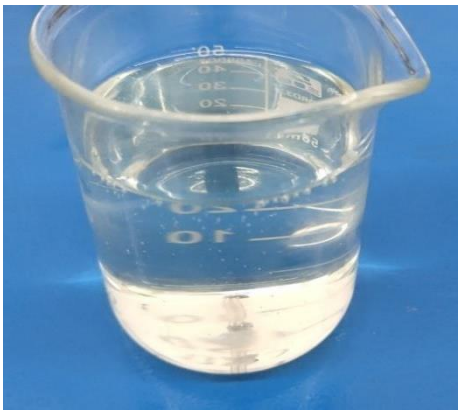

Figure 3.8 Commercial stabilizer

3.3 Methodology

This research focus of the thesis is the mechanical properties of the stabilized soils. By mixing and stirring the soil with different types of stabilizers (such as cement, fly ash, lime and gypsum), the physical and chemical reactions between soil, stabilizer and water would occur inside the samples to improve the strength of weak soil. By this way, the soil samples will be enhanced to meet the strength performance requirement of practical pavement embankment structure.

3.3.1 Overall research process

The first step of the research involves the identification of the key influencing factors on the strength of the stabilized soils. This will be carried out by conducting unconfined compressive strength tests on the stabilized fine soil and the stabilized dewatered soil A, respectively. The key influencing factors can be divided into four catalogues: stabilizer type and combination, initial moisture contents, sampling method and curing condition. Based on the results, selected stabilized dewatered soil A samples will be used to test for their California bearing ratio (CBR), triaxial shear strength and splitting strength, in order to study various aspects of the mechanical properties of the stabilized soil. Finally, the stabilized soil B will mainly be used to evaluate the possible influence of wetting-drying cycles, together with some comparisons. Table 3.7 shows overall test plan for this study. Detailed test information will be given in the next subsections.

For the pavement applications, the ABAQUS software will be used to simulate the behavior

of a pavement structure and its subgrade. Stabilized soils will be used to as subgrade materials. By using the results in the experiments, the mechanical properties of one proposed stabilized soil can be included in the analysis, together with information from ground investigation. The settlement and stability of the pavement subgrade can be finally evaluated. Figure 3.9 is the flow chart which shows the research process of this study.

Influence factors	Test method					
	UCS		SPT		CBR	Triaxial
Stabilizer type and combination	F	DA	DA	DB		
Moisture content	DA				DA	
Sampling method	F	DA				
Curing condition	F	DA	DB			DA
Wetting-drying cycles	DB					

F: fine soil; DA: dewatered drilling slurry - A; DB: dewatered drilling slurry - B

Table 3.7 Test plan of this study

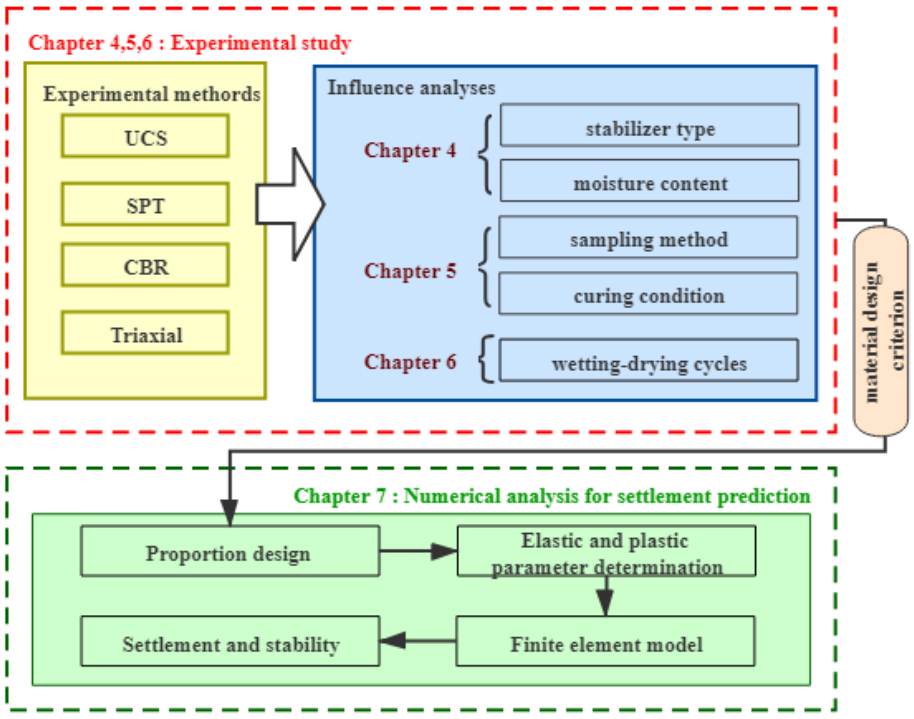

Figure 3.9 Research flow of this study

3.3.2 Unconfined compression test

Unconfined compression test in this study have been used to investigate the effects of all these influence factors (stabilizer type, moisture content, sampling method, curing condition and wetting-drying cycle) on the unconfined compressive strength of stabilized soil. For the part of stabilizer type, cement, lime, fly ash and gypsum would be used as stabilizers. They will be combined with different groups to investigate the effect of these stabilizer on unconfined compressive strength of stabilized soil. For the part of moisture content, the samples would be made up with moisture content of 18%, 22%, 26% and 30% to find the differences of these groups of samples. The part of sampling method and curing condition can be separated as several sections: the curing age, the curing age before compaction and the addition order of stabilizer. The curing age would be 7 days, 14 days and 28 days. The curing age before compaction means the pre-curing of cement-soil mixture before compaction, this curing age would be controlled as 0-7 hours. The addition order of stabilizer in this study means adding cement at first or later when preparing the mixture. The final part of wetting-drying cycle aims to investigate the effect of special treatment method on unconfined compressive strength of cement stabilized soil. The cycles would be varied from 0 to 4 to find the differences of strength caused by different cycles. Moreover, the samples also be prepared with moisture contents of 20%, 22%, 24% and 26%. The changes of strength for samples with different moisture contents under different wetting-drying cycles can be investigated.

3.3.3 CBR test

Some CBR tests were conducted in the present study to investigate the moisture content effect on the strength of stabilized soil. The CBR test samples were prepared with a constant cement content of 2% and a constant curing age of 7 days, and the moisture contents were prepared as 22%, 26% and 30%.

3.3.4 Triaxial shear test

Triaxial consolidated undrained shear test have been conducted in this study to investigate the

effects of stabilizer type and curing age on triaxial shear strength of stabilized soil. The soil samples would be stabilized with 3.5% cement or combination of 3.5% cement and 0,1% commercial stabilizer. The curing ages of these samples would be 7 days, 14 days and 28 days. Each group would be prepared with three samples, these test samples would be tested under cell pressures of 100 kPa, 200 kPa and 400 kPa. Three Mohr circles could be plotted and the envelope failure line can be obtained. The envelope line can be used to determine two shear strength indicators: the cohesion (c) and internal friction angle (φ) of the stabilized soil.

3.3.5 Splitting tension test

Splitting tension tests were performed to investigate the effects of commercial stabilizer, water soaking and curing age on indirect tensile strength of stabilized soil. The soil was stabilized by single cement (3.5%) or the combination of cement (3.5%) and commercial stabilizer (0.1%). The effect of water soaking was also studied. In addition, the samples were prepared with curing ages of 7 days, 14 days and 28 days to investigate the curing age effect.

Chapter 4: Effect of moisture content and stabilizer types

4.1 Introduction

In this chapter, unconfined compression tests and CBR tests have been conducted to investigate the effect of moisture content on the strength of cement stabilized soil. In the unconfined compression tests, the soil samples were prepared with a moisture content of 18%, 22%, 26% or 30%. In terms of the CBR tests, the samples were prepared with a moisture content of 22%, 26% or 30%. The effect of stabilizer types had been investigated by the unconfined compression test. In the test, cement, lime, fly ash and gypsum were used as stabilizers. Furthermore, the influencing degrees of these stabilizers were analyzed by grey correlation analyses.

4.2 Test procedures

4.2.1 Unconfined compression test procedures

For the unconfined compression test, the samples were prepared following the steps below:

(1) Soils from the construction site were ground into smaller assembles after drying by the oven in the laboratory for at least 8 hours, and then screened through a 0.2 mm sieve.

(2) The prepared soils were first well mixed with different stabilizers and then mixed with water by an electronic mixer.

(3) The mixture was compacted into a steel mold by layer (3 layers in total) within half an hour. The steel mold is shown in Figure 4.1. Each layer should be compacted about 40 times to make sure no further strain of the soil sample. And each layer interface was grooved after the compaction in order to connect layers tightly. The specimens were 50

mm in diameter and 100 mm in height.

(4) The soil sample was carefully removed from the steel mold by a hydraulic demolding instrument. Figure 4.2 shows the hydraulic demolding instrument.

(5) Once finished, the weights and heights of the samples were measured and recorded. Then, the samples were sealed and cured in the environmental cabinet with a constant temperature of 20℃ and a humidity of 95% for required curing ages. Figure 4.3 shows the environmental cabinet.

(6) After finishing the curing age, the unconfined compressive strengths of samples would be tested by MTS Model E45 tester which shows in Figure 4.4. The axial strain rate would be set up as 1 mm/min. When the peak values of stress-strain curves had been observed, ended the test, recorded the results and took photos of samples.

(7) In order to improve the accuracy of results, at least four parallel tests should be carried out in each group, and the average strength was finally taken as results for each group.

Figure 4.1 Steel mold for unconfined compression test sample

Figure 4.2 Hydraulic demolding instrument

Figure 4.3 Environmental cabinet

Figure 4.4 MTS Model E45

4.2.2 California Bearing Ratio test procedures

For the California bearing ratio test, the samples were prepared following the steps below:

(1) Soils from the construction site were ground into smaller assembles after drying by the oven in the laboratory for at least 8 hours, and then screened through a 20 mm sieve.

(2) The prepared soils were first well mixed with stabilizers and then mixed with water by an electronic mixer.

(3) The weight of the mould with sample was first measured. Then, fix the mould onto the bottom plate of the compaction instruction. According to the standard of heavy compaction test, a compaction hammer (4.5 kg) was installed and falling height was set to 45 cm.

(4) The CBR sample would be compacted layer by layer in 3 layers. The mass of the soil placed in Each layer is equal. Each layer was compacted 98 times Before putting in the next layer, the compacted surface was napped to ensure a good connection between two layers. The height of CBR sample was 116 mm and the diameter was 152 mm.

(5) Remove the sample with the mould form instruction mould carefully and seal it in a sample bag. The sealed sample (with mould) is cured in a curing environment at a temperature of 20 ℃ and a humidity of about 95%.

(6) For the cases that the soaking effect is not considered, the sample could be tested directed tested after the curing process. For the cases considering soaking effect, the specimen should be taken out from the curing chamber after curing and placed in the water tank for another 24 hours. The surface of the water surpasses the upper surface of the sample.

(7) The CBR tester is shown in Figure 4.5. The sample should be installed on the lift platform. Adjusting the penetration rod to a proper location to dock the top surface of the sample

(with a small load of around 45N), followed by adding 4 load plates around the penetration rod. The dial indicators are then zeroed.

(8) The load is applied in a loading rate of 1 mm/min. Readings of all three dial indicators are required to be recorded more than 5 times before a penetration distance of 2.5mm is reached.

Figure 4.5 CBR tester

4.3 Effect of moisture content

4.3.1 Unconfined compression test part

Dewatered drilling slurry - A was selected for this part of the study. Unconfined compression tests were carried out to investigate the effects of moisture content on the strength of stabilized soil. Cement was selected as the stabilizer. The cement contents were varied from 0 to 8 % for unconfined compression test samples. The curing age for all these samples was 7 days. Table 4.1 shows the experimental results of the UCS test.

Table 4.1 Experimental results of UCS test for moisture content

Sample	Cement content (%)	Moisture content (%)	UCS (MPa)
CE0-M18	0	18	0.274
CE2-M18	2	18	0.669

CE4-M18	4	18	1.053
CE6-M18	6	18	1.355
CE0-M22	0	22	0.104
CE2-M22	2	22	0.368
CE4-M22	4	22	0.565
CE6-M22	6	22	0.833
CE0-M26	0	26	0.078
CE2-M26	2	26	0.343
CE5.04-M26	5.04	26	0.475
CE7.56-M26	7.56	26	0.654
CE0-M30	0	30	0.018
CE1-M30	1	30	0.107
CE2-M30	2	30	0.164
CE4-M30	4	30	0.227
CE6-M30	6	30	0.347
CE8-M30	8	30	0.615

In total 18 groups of tests were carried out and the averaged UCS values were obtained. Figure 4.6 demonstrates that, for any given moisture content, there exists a proportional relationship between the 7-day unconfined compressive strength and the cement content. The moisture content has a significant effect on the unconfined compressive strength of stabilized soil samples. The largest unconfined compressive strength can be found when the moisture content is decreased to 18%. This is because this moisture content is close to the optimum moisture content which is 19.5% and the compacted sample is in a very dense condition. During the preparation of test samples, the change of moisture content mainly came from the quick reactions between cement and water, the effects of compaction and stabilization were limited. Hence, the effect of the change of moisture content on the strength of the stabilized soil was neglected in this study.

Failure modes of the specimens are also closely associated with the moisture content and the cement content. The dewatered slurry behaves plastically when the moisture content is relatively high. For instance, when the moisture content is 22%. Figure 4.7a demonstrates a shear failure mode with a large plastic deformation, in which the specimen bulges laterally into a ‘barrel shape’ at the beginning and generates a shear plane afterward. When the moisture content is decreased to 18%, a number of vertical cracks are generated during the compression

process as shown in Figure 4.7b, and the specimen fails in a semi-plastic mode instead, which is consistent with previous studies (Vallejo, 1988； Venkatramaiah, 1995). Undoubtedly, the stabilized soil could fail in a brittle mode if enough cement was added. In this study, since the cement content is relatively small compared to the corresponding moisture content, a semi-plastic failure mode is observed for the stabilized specimens, as shown in Figure 4.7c. Although both CE0-M18 and CE6-M18 failed in the same mode, the CE0-M18 behaves more like a plastic material, as there is no obvious peak in the stress-strain response curve as shown in Figure 4.8. Figure 4.8 also shows that as the cement content increases, the axial strain at the peak point becomes smaller and the stiffness tends to be higher.

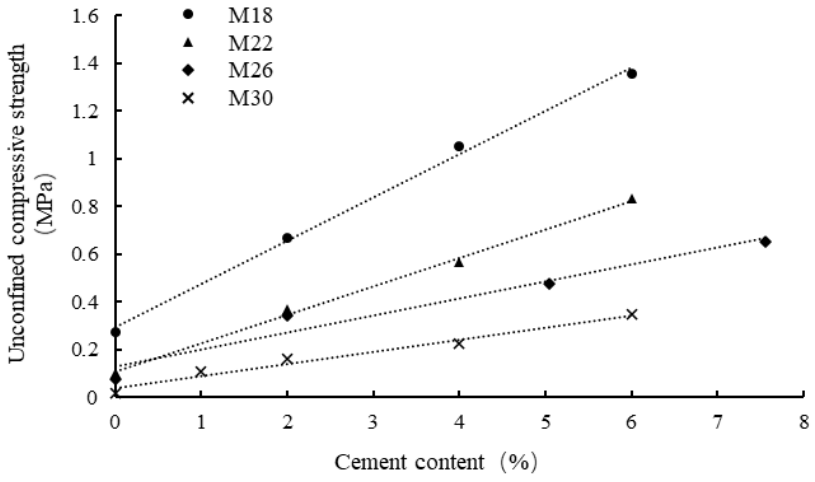

Figure 4.6 Effects of cement and moisture content on the 7-day UCS

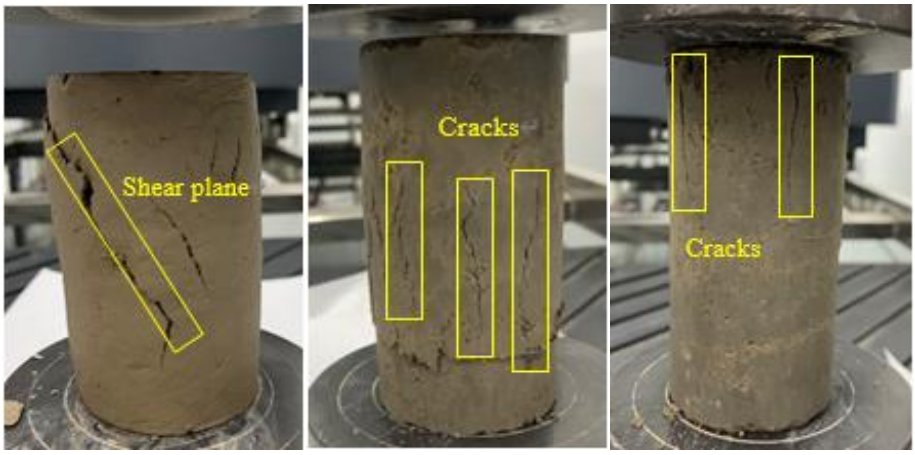

(a) CE0-M22 (b) CE0-M18 (c) CE6-M18

Figure 4.7 Failure mode

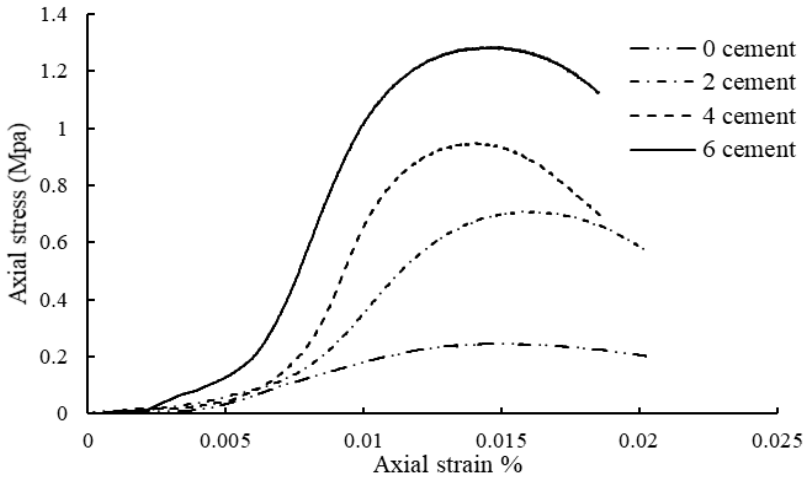

Figure 4.8 Stress-strain relationship for samples with a moisture content of 18%

Based on the data above, a contour plot (Figure 4.9) was developed, which shows the variation of unconfined compressive strength within practical ranges of moisture and cement contents in this study. As can be seen, the cement content has a more pronounced influence on the unconfined compressive strength when the moisture content approaches to optimum moisture content. despite of that, various combinations of cement and moisture contents could be chosen to achieve a specific strength. In practice, once the moisture content is obtained before the stabilization process, the required cement content can be efficiently determined in order to achieve a target 7-day unconfined compressive strength. In this work, the stabilized soils will be used as subgrade and embankment fill materials for an expressway, so the target unconfined compressive strength was set as 0.4 MPa.

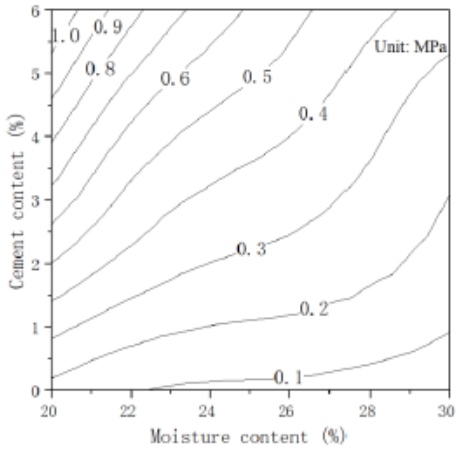

Figure 4.9 Contour of unconfined compressive strength

4.3.2 California Bearing ratio test part

Dewatered drilling slurry - A had been used for this part of the experiment. For CBR test samples, the cement content was a constant value of 2%. The moisture contents were changed from 18% to 30%. Curing ages for all these samples were 7 days. Table 4.2 shows the sample list for this part.

Table 4.2 Experimental results of CBR test for moisture content

Sample	Cement content (%)	Moisture content (%)	CBR (%)
CE2-M22	2	22	13.55
CE2-M26	2	26	11.7
CE2-M30	2	30	9.25

In pavement designs, a minimum CBR is usually required as an index of the subgrade soil strength. In China, the CBR value at the top of a pavement foundation should be no less than 8% for expressways; the CBR value for the embankment layer should be no less than 3% for lower embankment and 4% for the upper embankment layer (China Specifications, 2015). In this study, the influence of the moisture content on the CBR was also studied at the wet-side of the optimum moisture content. Figure 4.10 exhibits that the CBR decreases with the increasing moisture content, from 13.55% to 9.25%, in correspondence with the reduction of unconfined compressive strength from 0.37 MPa to 0.16 MPa. It should be noted that compared to non-stabilized soils, CBR values for chemically stabilized soils have less meaning

as a measure of strength (Nicholson et al., 1994). Nevertheless, it is still often used in the evaluation of the performance of stabilized soils for comparison purpose (de Figueirêdo Lopes Lucena et al., 2014).

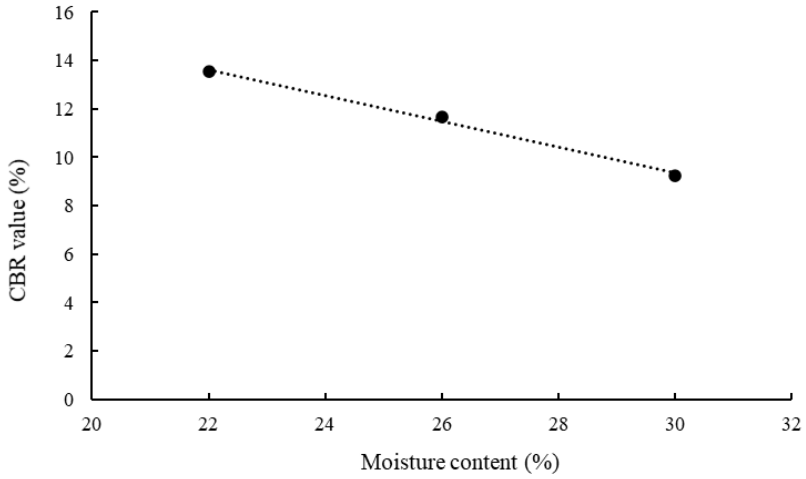

Figure 4.10 CBR after 7-day curing (cement content 2%)

4.4 Effect of stabilizers

4.4.1 Experimental results and discussion

The soil material used in this part of the experiments was the fine grain soil. In this study, cement, fly ash, lime and gypsum were used as the stabilizers. Their effects of different stabilizers on their contents on the unconfined compressive strength of the stabilized soil would be researched through quantitative analysis of the strength values. The moisture content of the fine grain soil was kept as 20% and the curing age for all samples was 7 days. And its UCS value was found to be 0.033 MPa. The test plan is shown in Table 4.3. And Figure 4.11 to Figure 4.17 shows the variation of UCS results with different contents of the stabilizers. Figure 4.18 shows the comparison of stress-strain curves of raw and stabilized soil samples.

Table 4.3 Test plan and UCS results for different stabilizers

Sample	CaO (%)	Fly ash (%)	Cement (%)	Gypsum (%)	UCS (MPa)	Increase percentage after	Group

						stabilization (%)	
CA2-FA4	2	4	0	0	0.183	454.5	I
CA2-FA6	2	6	0	0	0.248	651.5	I
CA2-FA8	2	8	0	0	0.32	869.7	I
CA2-FA10	2	10	0	0	0.194	487.9	II
CA2-FA12	2	12	0	0	0.209	533.3	II
CA4-FA8	4	8	0	0	0.256	675.8	II
CA4-FA12	4	12	0	0	0.255	672.7	II
CA4-FA16	4	16	0	0	0.274	730.3	II
CA6-FA12	6	12	0	0	0.306	827.3	II
CA6-FA18	6	18	0	0	0.327	890.9	II
CA6-FA24	6	24	0	0	0.308	833.3	I
CA2-FA4-CE2	2	4	2	0	0.326	887.9	I
CA2-FA4-CE3	2	4	3	0	0.451	1266.7	I
CA2-FA4-CE4	2	4	4	0	0.6	1718.2	I
CA2-FA4-CE2-CAS0.5	2	4	2	0.5	0.367	1012.1	I
CA2-FA4-CE2-CAS1	2	4	2	1	0.378	1045.5	I
CA2-FA4-CE2-CAS1.5	2	4	2	1.5	0.431	1206.1	I
CA2-FA4-CE2-CAS2	2	4	2	2	0.464	1306.1	I
CA2-FA4-CE2-CAS3	2	4	2	3	0.442	1239.4	II
CA2-FA4-CE2-CAS4	2	4	2	4	0.469	1321.2	II
CA2-FA4-CE2-CAS5	2	4	2	5	0.444	1245.5	II
CA3-FA6-CE2-CAS1	3	6	2	1	0.522	1481.8	I
CA3-FA6-CE3-CAS1	3	6	3	1	0.542	1542.4	I
CA4-FA8-CE2-CAS1	4	8	2	1	0.582	1663.6	I
CA4-FA8-CE4-CAS1	4	8	4	1	0.927	2709.1	I

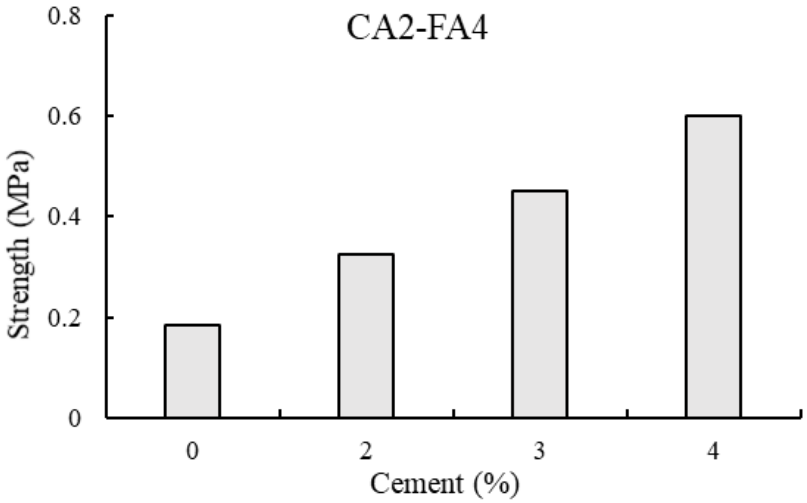

Figure 4.11 Influence of cement on UCS of fine grained soil

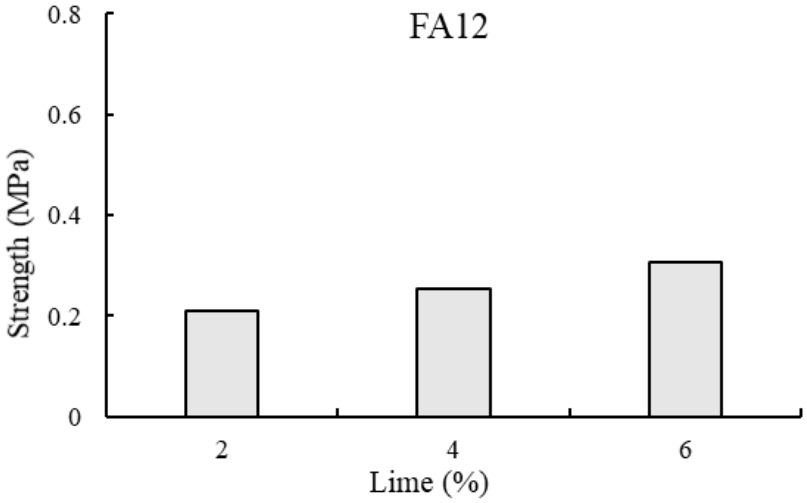

Figure 4.12 Influence of lime on UCS of fine grained soil

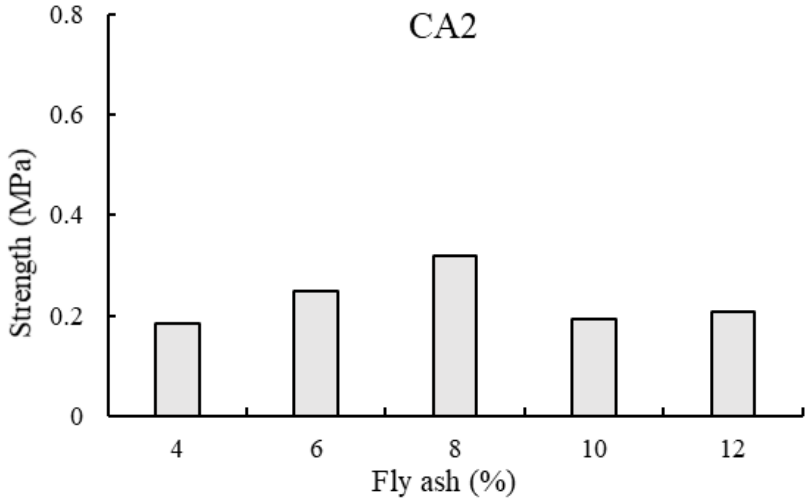

Figure 4.13 Influence of fly ash on UCS of fine grained soil

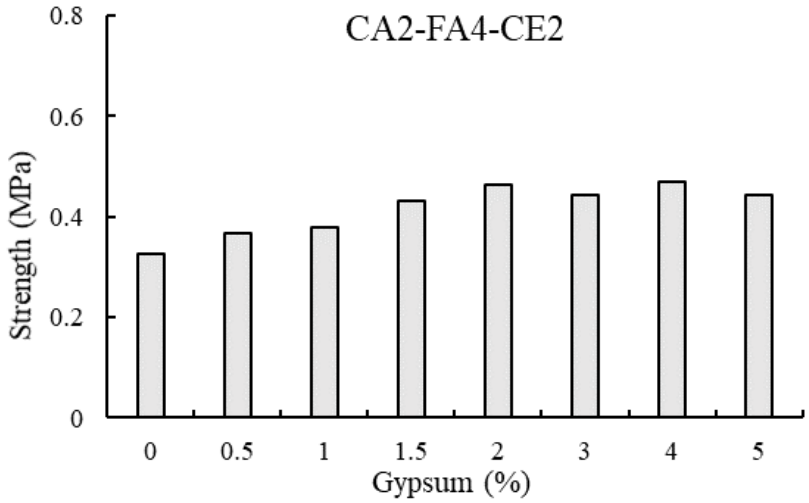

4.14 Influence of gypsum on UCS of fine grained soil

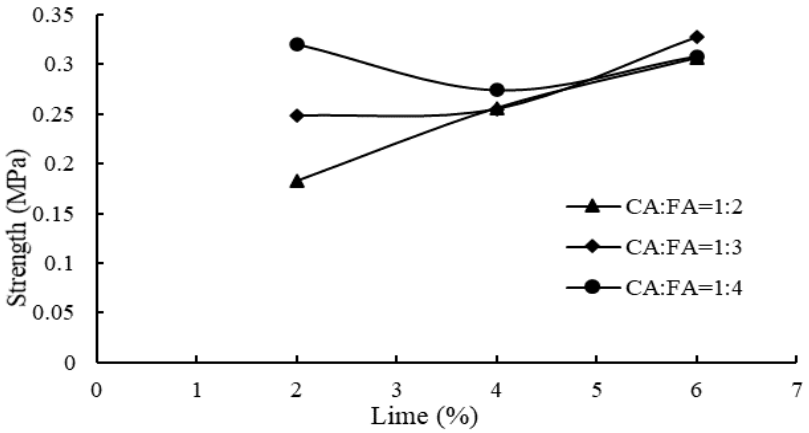

Figure 4.15 Influence of fly ash/ lime ratio on UCS of fine grained soil

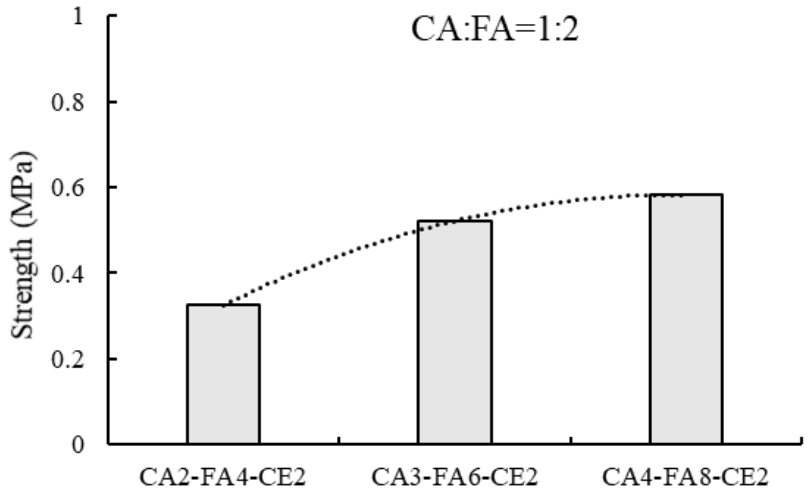

Figure 4.16 Influences of different proportions of stabilizers on UCS when lime: fly ash = 1: 2

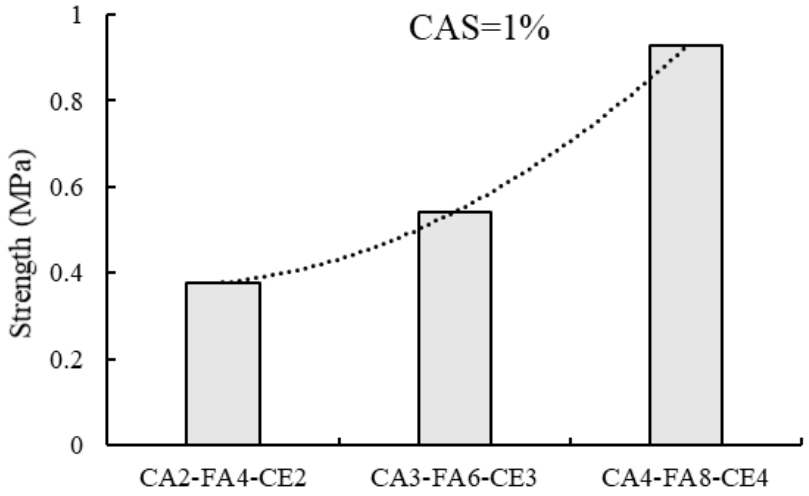

Figure 4.17 Influence of different proportions of stabilizers on UCS when gypsum = 1%

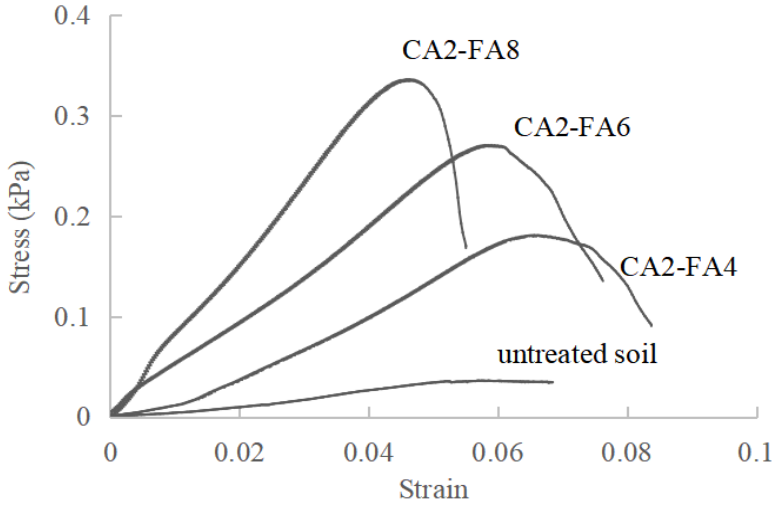

Figure 4.18 Stress-strain curves for raw and stabilized soils

As can be seen in Figure 4.11, for given lime and fly ash contents, when the cement content was changed from 2% to 4%, the unconfined compressive strength was proportionally increased by a magnitude of 274 kPa. This linear relationship is consistent with previous findings (Pandey and Rabbani, 2017). When the cement content was increased from 0% to 2%, the unconfined compressive strength was raised by 143 kPa.

Compared to cement, the influence of lime and fly ash contents are relatively small. For instance, by increasing the lime or fly ash content from 4% to 6%, the unconfined compressive strength is raised by 51 kPa (Figure 4.12) and 65 kPa (Figure 4.13) respectively. Moreover, for a given lime content, there exists an optimum fly ash content that can maximize the unconfined compressive strength, which agrees with Kumar et al. (2007)'s finding. It is further found that when the lime content was relatively high, the influence of the fly ash content became limited, as shown in Figure 4.15; and therefore the increase of unconfined compressive strength in these cases is mainly attributed to the rise of the lime content. It can also be inferred from Figure 4.16 that the effect of cement is higher than the overall effect of lime and fly ash, since the growth trend of the unconfined compressive strength is changed from deceleration to acceleration due to some additional cement.

The influence of gypsum is demonstrated in Figure 4.14. It can be known that the strengths of the materials have been enhanced due to the addition of gypsum and an optimum content of gypsum is observed, above which the strength starts to decrease with the increasing

gypsum content. Huang and Hu (1998), Guo (2007), Huang et al. (2007) and Jin et al. (2014) had similar findings and explained that the excessive expansion of ettringites in gypsum is slow in the stabilized soil; if excess gypsum is added, the unreacted gypsum may weaken the bonds between soil particles and the cementitious compounds due to the platy shape of gypsum particles (Kumar et al., 2007； Kolay and Pui, 2010). When the gypsum content was increased from 0% to 2%, the unconfined compressive strength was raised by 138 kPa, which is lower than those of cement but higher than those of lime and fly ash.

It can be concluded from the above quantitative analyses that the cement has the most obvious effect on the unconfined compressive strength and the addition of gypsum can further increase the strength effectively. The effect of fly ash is limited, especially when the lime content is high. Also, increasing the lime content alone could not affect the strength obviously. Moreover, it was found that a higher stabilizer content is normally in correspondence to higher stiffness and a smaller deformation at failure, as shown in typical stress-strain curves in Figure 4.18. Also note that the effects of fly ash and lime on the unconfined compressive strengths could become more obvious if a longer curing age is considered as the hydration reaction rate for fly ash and pozzolanic reaction rate for lime are slow. Therefore, even though the effects of lime and gypsum are limited, their effectiveness on the long-term strength of stabilized soil samples need further assessment in the future by considering curing ages.

4.4.2 Grey correlation analysis

4.4.2.1 introduction of grey correlation analysis

Grey correlation analysis is a data process method developed based on geometrical mathematics, for which black represents having no information between two sequences while white represents having all information. Accordingly, the grey system represents a level of information between black and white. By using the grey correlation analysis, the grade of correlation between two sequences can be determined, known as the grey correlation coefficient (Deng, 1989； Gau et al., 2006). The grey correlation analysis has been widely used for analyzing the relationship between sequences with fewer data and evaluates the

effectiveness of each sequence on the target sequence by ranking the grey correlation coefficient. In the field of civil engineering, this method has been applied by researchers to study the impact degrees of different factors on a target objective, thus providing guidance for engineering applications. For instance, Wang et al. (2004) studied the correlations between the stability of slide slopes and some sensitive factors. They found that the effects of cohesion and friction angle of the materials are more significant than those of earthquake acceleration and water level in reservoirs. For a cut-and-fill pavement foundation, Su et al. (2012) ranked the relations between the slope stability and possible influencing factors, including the properties of fills and the geometry of the embankment slope. He et al. (2014) investigated the effect of particle characteristics on the compressive strength for lightweight aggregate concretes and provided suggestions on the optimization strategy based on the grey relational analyses. Zhang and Zhang (2007) considered the effect of different particle fractions of slag powders on the strength of slag cements, and suggestions were proposed to help the slag cement to gain more strength.

It is worth mentioning that one important process in the grey relational analysis is the normalization of source data since the comparative sequences usually have different dimensions and their numerical values may vary greatly. Several different normalization methods have been used in the previous researches, such as range method (Su et al., 2012), average range method (Zhang and Zhang, 2007; He et al., 2014), maximization or minimization methods (Mishra et al., 2015) and initialization method (Feng et al., 2014). Despite of those applications, none of the researches has examined the effects of different normalization methods on the grey relational analysis results. Also, the applicability of the grey relational analysis in identifying the impact degree of various stabilizers on the soil strength is yet to be investigated.

In this study, cement, fly ash, lime and gypsum have been used as the stabilizers for a fine soil. Their effects on the UCS of the stabilized soil will be researched through both quantitative analysis and grey correlation analysis. The influence of various normalization methods will also be studied.

4.4.2.2 Application of grey correlation analysis

In the grey relational analysis system, the UCSs in Table 4.1 were used as the reference sequence $y_0(j) = \{y_0^1, y_0^2, \dots, y_0^m\}$, where m represents the number of the group tests. Meanwhile, the contents of the four stabilisers were set as comparison sequences $y_i(j) = \{y_i^1, y_i^2, \dots, y_i^m\}$, where i = 1, 2, …, n, representing the reference number of each stabiliser.

Following that, each sequence should be scaled using one normalisation method in order to eliminate the effect of various ranges of different sequences. In this study, five common-used normalisation methods (Equation 4.1 - 4.5) were considered and the most effective one can be determined referring to the quantitative analyses. Note that, among those methods, the maximisation method will lead to an infinite value of $x_i(j)$, thus will not be used in the following analysis.

(1) Initialization:

$$x_i(j) = \frac{y_i(j)}{y_i(1)}, y_i(1) \neq 0$$

Equation 4.1 Initialization method

(2) Average:

$$x_i(j) = \frac{y_i(j)}{\bar{y}_i}, \qquad \bar{y}_i = \frac{1}{n}\sum_{k=1}^{n} y_i(j)$$

Equation 4.2 Average method

(3) Range:

$$x_i(j) = \frac{y_i(j) - \min[y_i(j)]}{\max[y_i(j)] - \min[y_i(j)]}$$

Equation 4.3 Range method

(4) Maximisation:

$$x_i(j) = \frac{y_i(j)}{\min\,[y_i(j)]}$$

Equation 4.4 Maximization method

(5) Minimisation:

$$x_i(j) = \frac{y_i(j)}{\max\,[y_i(j)]}$$

Equation 4.5 Minimization method

Then, the absolute difference of sequences of x_0 and x_i were calculated using Equation 4.6 in which the reference sequence $x_0(j)$ for each normalisation method is the corresponding unconfined compressive strength sequence in Table 4.5.

$$\Delta_i(j) = |x_0(j) - x_i(j)|$$

Equation 4.6 Absolute difference of sequences

Based on those, the maximum and minimum values of $\Delta_i(j)$ were obtained:

$$\Delta_{max} = \max_i \max_j [\Delta_i(j)]$$

Equation 4.7 Maximum value of $\Delta_i(j)$

$$\Delta_{min} = \min_i \min_j [\Delta_i(j)]$$

Equation 4.8 Minimum value of $\Delta_i(j)$

And the relational coefficient of each test was calculated:

$$\xi_i(k) = \frac{\Delta_{min} + \rho\Delta_{max}}{\Delta_i(j) + \Delta_{max}}$$

(where ρ is a resolution coefficient, between 0 and 1, normally taken as 0.5)

Equation 4.9 Relational coefficient calculation

Finally, the relevancy of each factor (stabiliser content) was obtained by calculating the relational coefficient:

$$r_i = \frac{1}{n}\sum_{k=1}^{n} \xi_i(k)$$

Equation 4.10 Relevancy of each factor

For the cases in this study, relational coefficients obtained using different normalization methods are displayed in Table 4.4 and compared in Figure 4.19. Normally, a factor is considered to be more influential on the reference value if its relational coefficient is relatively high (Yaragal et al., 2020). Therefore, the order of the impact degree of various factors on the UCS can be obtained, as shown in Table 4.5. It can be seen that by using different normalization methods, the orders of stabilizers show different. Using the average method, it appears that the effect of cement content is smaller than that of lime content, which is contradictory to the quantitative analysis. Results in Table 4.5 shows that either fly ash or gypsum has the lowest influence on the UCS. One possible reason is that the effects of fly ash and gypsum on the UCS are not always positive. Optimum contents can be observed in Figure 4.13 and Figure 4.14. Therefore, Grey relational analyses were further carried out by only using the data within the increased stage. All test results in Table 4.4 were divided into two groups. Group I refers to the cases where the rise of the stabilizer content has a clear positive impact, while Group II represents the rest. Accordingly, the relational coefficients and the orders of impact were obtained and shown in Table 4.6. It is clear that the order obtained by using the range method is more reasonable when compared with the quantitative analysis.

Sample	Initialization					Average					Range					Minimization				
	CE	CA	FA	CAS	UCS	CE	CA	FA	CAS	UCS	CE	CA	FA	CAS	UCS	CE	CA	FA	CAS	UCS
CA2-FA4-CE2-CAS0.5	1	1	1	1	1	1.47	0.68	0.51	0.6	0.93	0.50	0	0	0.1	0.25	0.5	0.33	0.17	0.1	0.40
CA2-FA4-CE2-CAS1	1	1	1	2	1.03	1.47	0.68	0.51	1.19	0.96	0.50	0	0	0.2	0.26	0.5	0.33	0.17	0.2	0.41
CA2-FA4-CE2-CAS1.5	1	1	1	3	1.18	1.47	0.68	0.51	1.79	1.10	0.50	0	0	0.3	0.33	0.5	0.33	0.17	0.3	0.46
CA2-FA4-CE2-CAS2	1	1	1	4	1.27	1.47	0.68	0.51	2.38	1.18	0.50	0	0	0.4	0.38	0.5	0.33	0.17	0.4	0.5
CA2-FA4-CE2-CAS3	1	1	1	6	1.21	1.47	0.68	0.51	3.57	1.13	0.50	0	0	0.6	0.41	0.5	0.33	0.17	0.6	0.48
CA2-FA4-CE2-CAS4	1	1	1	8	1.28	1.47	0.68	0.51	4.76	1.19	0.50	0	0	0.8	0.44	0.5	0.33	0.17	0.8	0.51
CA2-FA4-	1	1	1	10	1.21	1.47	0.68	0.51	5.95	1.13	0.50	0	0	1	0.41	0.5	0.33	0.17	1	0.48

CE2-CAS5																			
CA3-FA6-CE2-CAS1	1	1.5	1.5	2	1.42	1.47	1.01	0.76	1.19	1.33	0.50	0.25	0.1	0.2	0.46	0.5	0.5	0.25	0.2	0.56
CA3-FA6-CE3-CAS1	1.5	1.5	1.5	2	1.48	2.21	1.01	0.76	1.19	1.38	0.75	0.25	0.1	0.2	0.48	0.8	0.5	0.25	0.2	0.58
CA4-FA8-CE2-CAS1	1	2	2	2	1.59	1.47	1.35	1.01	1.19	1.48	0.50	0.50	0.2	0.2	0.54	0.5	0.67	0.33	0.2	0.63
CA4-FA8-CE4-CAS1	2	2	2	2	2.53	2.94	1.35	1.01	1.19	2.36	1	0.50	0..2	0.2	1	1	0.67	0.33	0.2	1
CA2-FA4	0	1	1	0	0.50	0	0.68	0.51	0	0.46	0	0	0	0	0	0	0.33	0.17	0	0.2
CA2-FA6	0	1	1.5	0	0.68	0	0.68	0.76	0	0.63	0	0	0.1	0	0.09	0	0.33	0.25	0	0.27
CA2-FA8	0	1	2	0	0.87	0	0.68	1.01	0	0.81	0	0	0.2	0	0.18	0	0.33	0.33	0	0.34
CA2-FA10	0	1	2.5	0	0.53	0	0.68	1.26	0	0.49	0	0	0.3	0	0.02	0	0.33	0.42	0	0.21
CA2-FA12	0	1	3	0	0.57	0	0.68	1.52	0	0.53	0	0	0.4	0	0.04	0	0.33	0.5	0	0.23

CA4-FA8	0	2	2	0	0.70	0	1.35	1.01	0	0.65	0	0.50	0.2	0	0.10	0	0.67	0.33	0	0.28
CA4-FA12	0	2	3	0	0.69	0	1.35	1.52	0	0.65	0	0.50	0.4	0	0.10	0	0.67	0.5	0	0.27
CA4-FA16	0	2	4	0	0.75	0	1.35	2.02	0	0.70	0	0.50	0.6	0	0.12	0	0.67	0.67	0	0.3
CA6-FA12	0	3	3	0	0.83	0	2.03	1.52	0	0.78	0	1	0.4	0	0.17	0	1	0.5	0	0.33
CA6-FA18	0	3	4.5	0	0.89	0	2.03	2.27	0	0.83	0	1	0.7	0	0.19	0	1	0.75	0	0.35
CA6-FA24	0	3	6	0	0.84	0	2.03	3.03	0	0.78	0	1	1	0	0.17	0	1	1	0	0.33
CA2-FA4-CE2	1	1	1	0	0.89	1.47	0.68	0.51	0	0.83	0.50	0	0	0	0.19	0.5	0.33	0.17	0	0.35
CA2-FA4-CE3	1.5	1	1	0	1.23	2.21	0.68	0.51	0	1.15	0.75	0	0	0	0.36	0.8	0.33	0.17	0	0.49
CA2-FA4-CE4	2	1	1	0	1.64	2.94	0.68	0.51	0	1.53	1	0	0	0	0.56	1	0.33	0.17	0	0.65

Table 4.4 Normalized data by using four common-used normalization method

Table 4.5 Correlation coefficients

Normalization	CA	FA	CE	CAS	Order of impact on UCS
Initialization	0.891	0.835	0.910	0.790	CE>CA>FA>CAS
Average	0.842	0.787	0.815	0.746	CA>CE>FA>CAS
Range	0.609	0.595	0.757	0.707	CE>CAS>CA>FA
Minimization	0.700	0.621	0.723	0.569	CE>CA>FA>CAS

Table 4.6 Correlation coefficients for increase stage

Normalization	CA	FA	CE	CAS	Order of impact on UCS
Initialization	0.949	0.930	0.930	0.833	CA>CE≈FA>CAS
Average	0.946	0.920	0.911	0.799	CA>FA>CE>CAS
Range	0.655	0.653	0.734	0.710	CE>CAS>CA≈FA
Minimization	0.770	0.733	0.752	0.617	CA>CE>FA>CAS

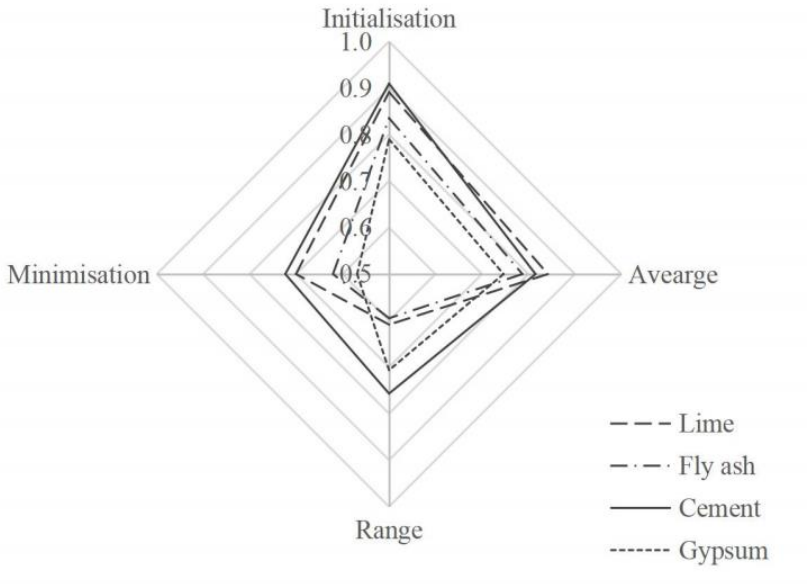

Figure 4.19 Comparison of correlation coefficients for different normalization methods and stabilizers

4.5 Summary

This effect of moisture content has been investigated in this chapter. Both UCS and CBR tests show that the stabilized soil sample would have the largest strength when the moisture content close to the optimum moisture content. At the dry side of the optimum moisture content, the strength would have an increasing trend; at the wet-side of the optimum moisture content, the

strength would have a decreasing trend.

This chapter also investigates the effects of four stabilizers on the unconfined compressive strength of a stabilized fine grain soil using quantitative analyses. In the quantitative analysis, it is found that there exists a positive linear relationship between cement content and the unconfined compressive strength. the effect of the cement content on the unconfined compressive strength is higher than gypsum, followed by lime and fly ash. For both fly ash and gypsum, there exist optimum contents that can maximize the unconfined compressive strengths. A contour plot is further developed which can guide the selection of the stabilization strategy considering in-situ moisture content. This is then used to determine the cement content for the treatment of the waste drilling slurry in an on-site plant.

In grey correlation analysis, the selection of normalization method can change the correlation ranking of the stabilizers with respect to unconfined compressive strength. In this study, the analysis using the range normalization method gives a reasonable ranking of the stabilizers, whereas the average method is not applicable. The order of impact is also affected by the changing trend of the unconfined compressive strength, which is not explicitly shown in the calculated relational coefficients. Therefore, grey correlation analysis should be conducted with care when a change of trend is possible. It can be further concluded that cement is the most effective stabilizer for the fine grain soil. An addition of a proper content of gypsum can further increase the strength. The effects of quick lime and fly ash are limited on the early-stage (7 days) strength, but their influences on the long-term strength need further assessments.

Chapter 5: Effect of sampling and curing conditions

5.1 Introduction

In this chapter, unconfined compression tests were conducted to investigate the effect of both sampling conditions and curing conditions. The UCS samples were stabilized by cement only. In addition, splitting tension tests and triaxial shear tests were conducted to investigate the effect of the curing age on the strength of stabilized soil. These samples were stabilized by cement (3.5%) only or a combination of cement (3.5%) and commercial stabilizer (0.1%).

5.2 Test procedures

The test procedures of the unconfined compression test and CBR test have been introduced in the previous chapter 4. This following subsection introduces the test procedures of triaxial shear test and splitting tension tests.

5.2.1 Triaxial shear test (consolidated undrained) procedures

For the triaxial shear test, the samples were prepared following the steps below:

(1) The triaxial sample preparation method and curing condition is same to that of UCS sample.

(2) The sample was installed into a rubber membrane, and seal the two ends by O-rings. Followed by installing the specimen into the triaxial chamber. Figure 5.1 shows the components of the triaxial tester.

(3) The chamber would be injected with water until the water surface over the specimen cap.

(4) The cell pressure is applied by controlling the pressure controller in the software. The

drain valve should be opened after then for the consolidation of the specimen until the axial strain of the specimen becomes stable.

(5) As undrained tests are conducted, the drain valve should be closed after consolidation, but before compression. A shearing rate of 0.1 mm/min is applied. The test could be terminated when a peak axial stress is obtained or the axial strain reaches 15% . The test data should be recorded after the test.

(6) Finally, all the pressures are removed after the test. Water in the chamber should be drained clearly before removing the triaxial chamber form the instrument. The last step is to remove the specimen and clean the instrument.

Figure 5.1 Triaxial tester

5.2.2 Splitting tension test procedures

The sample preparation method of splitting tension test is similar to that of UCS but with a larger dimension. Both the height and diameter of the sample was 100 mm. Soaking and non-soaking conditions are considered before testing. The soaking process is similar to that described in the Subsection 5.2.1 for CBR tests. Splitting fixture is installed on the MTS Model E45 for the test. The loading rate is 1 mm/min. Each test could be ended when the radial stress reaches a peak value.

5.3 Effect of curing age

5.3.1 Triaxial shear test

Dewatered drilling slurry - A was selected as soil material for the triaxial shear test. The soil samples were stabilized by cement (CE3.5) or the combination of cement and commercial stabilizer (CE3.5-C0.1). The curing ages varied from 7 to 28 days. All the stabilized soil samples were prepared with a constant moisture content of 26%. The cell pressures used in this study were 100, 200 and 400 kPa. Table 5.2 shows the test plan and results for the triaxial shear test. c indicates the cohesion and φ indicates the internal friction angle.

Table 5.1 Test plan and results of triaxial shear test

Sample	Cement content (%)	Commercial stabilizer content (%)	Curing age (d)	Moisture content (%)	c (kPa)	φ (°)
CE3.5-M26-T7	3.5	/	7	26	135	22.5
CE3.5-C0.1-M26-T7	3.5	0.1	7	26	130	25.5
CE3.5-M26-T14	3.5	/	14	26	150	26
CE3.5-C0.1-M26-T14	3.5	0.1	14	26	115	26.5
CE3.5-M26-T28	3.5	/	28	26	224	26.5
CE3.5-C0.1-M26-T28	3.5	0.1	28	26	160	27

Some findings could be concluded from Table 5.1:

(1) The addition of the commercial stabilizer causes an almost linear decrease of the cohesion with the increase of the curing age.

(2) The addition of commercial stabilizer caused the increase of the internal friction angle. The internal friction angle increases by 3° for 7-day samples and 0.5° for both 14-day and 28-day samples. The larger increment in the first 7 days might be caused by the quick hydration and pozzolanic reactions at the beginning. Over a longer period, the strength of the sample tends to be stable and the change of the internal friction angle became smaller. Nevertheless, the effect of curing age on the internal friction angle of the stabilized soil is

limited.

(3) Curing age has a significant effect on the cohesion for both CE stabilized samples and CE-C stabilized samples. With the curing age increases from 7 days to 28 days, the cohesion is increased by 89 kPa and 30kPa, respectively. More obvious changes could be observed at the early curing ages.

Figure 5.2 shows the relationships between the deviatoric stresses and the axial strain for 7-day, 14-day and 28-day cured samples. The peak value of the deviatoric stress increases with the increase of the cell pressure. The increment indicates that the increasing cell pressure can improve the strength of stabilized soil. Furthermore, the failure strain also increased with the increase of the cell pressure. Comparing the data in Figure 5.2(a), (b) and (c), the increasing of curing age leads to larger peak deviatoric stresses. Compared the peak deviatoric stresses of CE3.5 with those of CE3.5-C0.1, the addition of the commercial stabilizer improves the strength of the stabilized soil sample significantly.

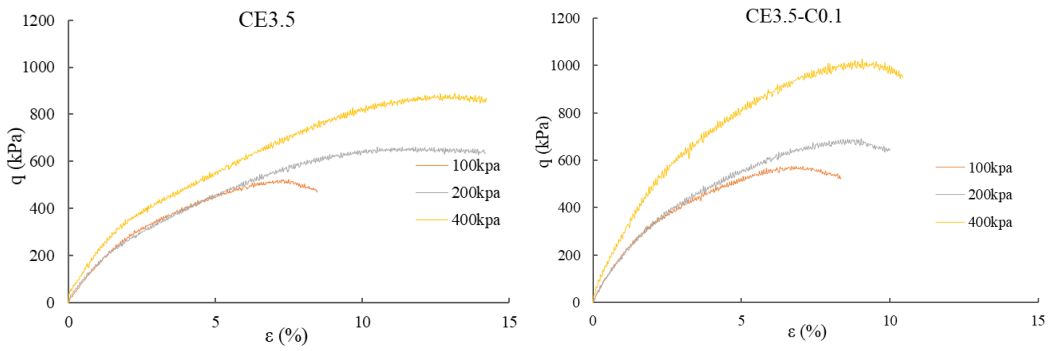

(a) Relationship between principal stress and axial strain (7 days)

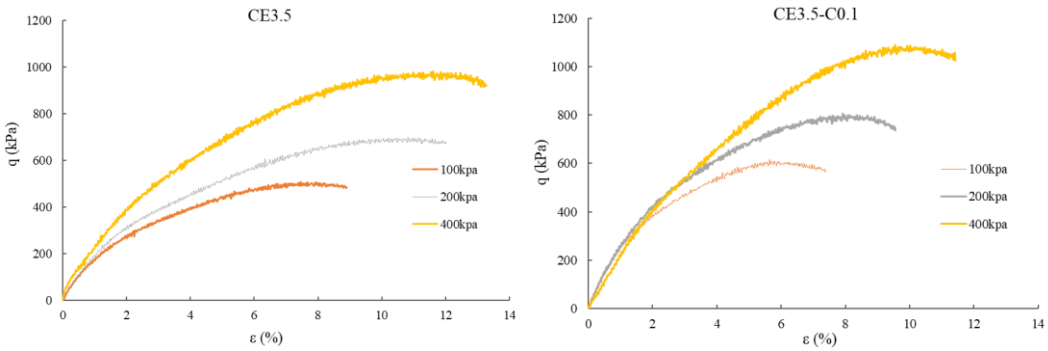

(b) Relationship between principal stress and axial strain (14 days)

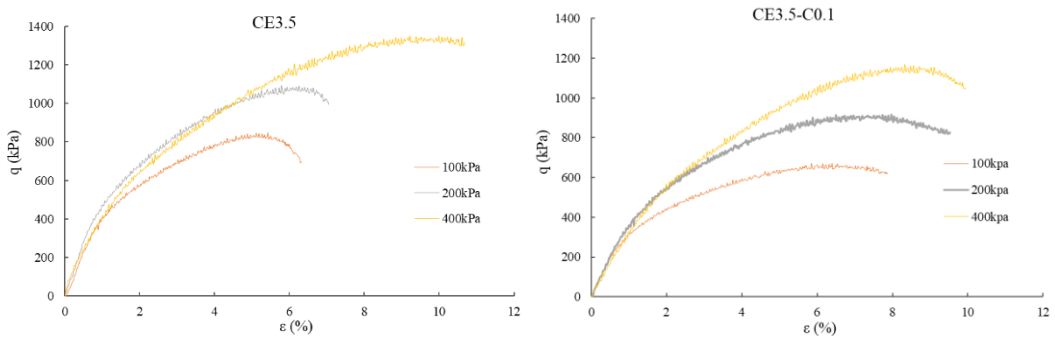

(c) Relationship between principal stress and axial strain (28 days)

Figure 5.2 Relationship between deviatoric stress and axial strain

Both the UCS test results and triaxial tests results are used for plotting the Mohr circles and determining the cohesion and friction angle in the present study. An example is given in the Figure 5.4, a well matching line can be obtained. It should be noted that the tensile strength (0.315 MPa) can be roughly estimated from this figure, which will be compared with the numerical analysis results to verify the feasibility of an embankment with stabilized soil.

Figure 5.4 shows the failure modes of CE3.5 samples after different during ages. It can be seen that the 7-day sample has an obvious drum shaped mode failure. The 14-day sample has a drum shaped failure as well, but also show a clear shear plane. For the 28-day sample, the failure mode changes to an obvious brittle failure. Hence, it can be concluded that with the increasing of curing age, the failure modes could transfer from drum shaped failure to brittle failure gradually.

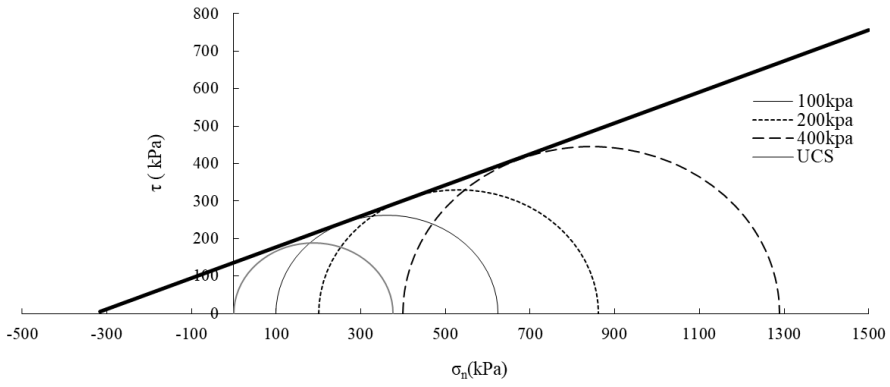

Figure 5.3 Results comparison between UCS and triaxial test for CE3.5-M26-T7 sample

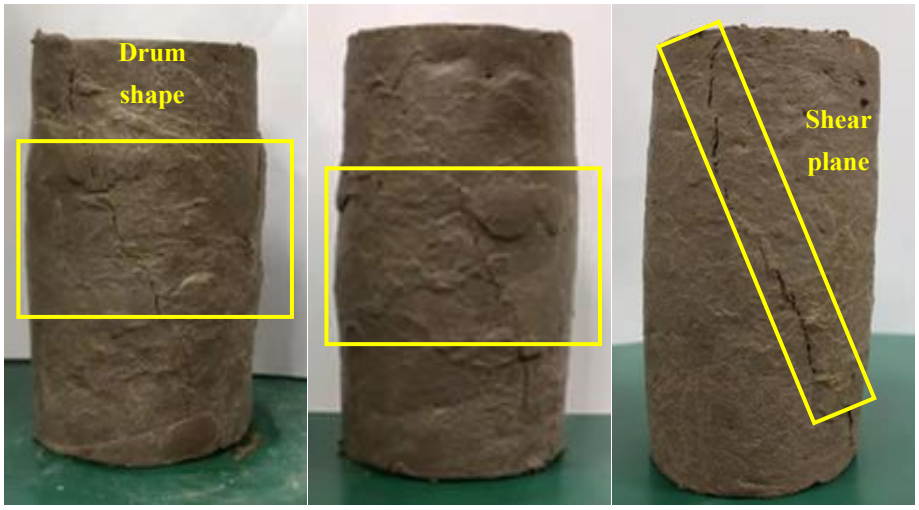

(a) 7 days curing (b) 14 days curing (c) 28 days curing

Figure 5.4 Failure mode of CE3.5 samples

5.3.2 Unconfined compression test

In this subsection, UCS tests were carried out for stabilized soil with different initial moisture content (20%, 22%, 24% and 26%). The effect of different curing ages were also investigated. All the tests are listed in Table 5.2 and the results are given in Figure 5.5.

Table 5.2 Test plan and UCS results for curing age

Sample	Moisture content (%)	Curing age (d)	UCS (MPa)
CE3.5-M20-T7	20	7	0.588
CE3.5-M20-T14	20	14	0.620
CE3.5-M20-T28	20	28	0.676
CE3.5-M22-T7	22	7	0.403
CE3.5-M22-T14	22	14	0.459
CE3.5-M22-T28	22	28	0.547
CE3.5-M24-T7	24	7	0.248
CE3.5-M24-T14	24	14	0.320
CE3.5-M24-T28	24	28	0.384
CE3.5-M26-T7	26	7	0.215
CE3.5-M26-T14	26	14	0.280
CE3.5-M26-T28	26	28	0.355

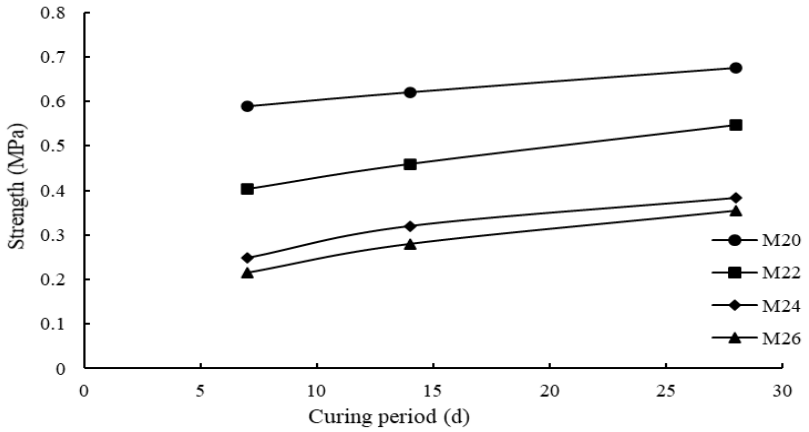

Figure 5.5 Influence of curing age on UCS of dewatered drilling slurry - A

According to Figure 5.5, the sample with a moisture content of 20% has the largest UCS value, this could because the optimum moisture content is around 19.5%. With an increase of moisture content from 20% to 26%, the strength decreases gradually. For each group of samples, the strength trends to linearly grow with the increasing of curing age. The test results agree with other researches' finding.

5.3.3 Splitting tension test part

This part of experiment selected dewatered drilling slurry - B as the soil material. Cement and commercial stabilizer were used as the stabilizers. And the curing ages of these samples were 7, 14 and 28 days. For 7-day samples, the effect of water soaking on the splitting tensile strength of soil was be investigated. Table 5.3 shows the test samples for this part of study.

The splitting tensile strength can be calculated based on the Equation 5.1 according to the test results

$$R_i = \frac{2P}{\pi dh}\left(sin2\alpha - \frac{a}{d}\right) = 0.006263\frac{P}{h}$$

In this equation: R_i – splitting tensile strength (MPa); d – diameter of the sample (mm); a – width of the bar (mm); α – radius angle corresponding to the bar (°); P – the maximum radial force at sample failure (N); h – the height of unsoaked or soaking sample (mm).

Equation 5.1 Splitting tensile strength calculation

Table 5.3 Test plan and results of splitting tension test

Sample	Cement content (%)	Commercial stabilizer content (%)	Curing age (d)	Splitting tensile strength (MPa)
CE3.5-M26-T7-W1	3.5	0	7	0.021
CE3.5-M26-T7	3.5	0	7	0.028
CE3.5-C0.1-M26-T7-W1	3.5	0.1	7	0.021
CE3.5-C0.1-M26-T7	3.5	0.1	7	0.071
CE3.5-C0.1-M26-T14-W1	3.5	0.1	14	0.028
CE3.5-C0.1-M26-T28-W1	3.5	0.1	28	0.04

According to Table 5.3, some findings can be concluded as below:

(1) For cement stabilized samples, the effect of water soaking on the splitting tensile strength is significant. The strength decreases by 25% from 0.028 MPa to 0.021 MPa. The results could reflect the weak water stability of the stabilize sample. It can be inferred than longer curing age could lead to stronger water stability, but needs further studies.

(2) Compare the 7-day sample stabilized by cement with 7-day sample stabilized by both cement and commercial stabilizer, the splitting tensile strength increased from 0.028 MPa to 0.071 MPa because of the addition of commercial stabilizer. In light of this increment, it could be found that commercial stabilizer has a great effect on improving the splitting tensile strength of stabilized soil.

(3) For samples stabilized by both cement and commercial stabilizer, the effect of water soaking on the splitting tensile strength becomes more obvious comparing with that of cement stabilized sample. The splitting tensile strength is decreased by 70% from 0.071 MPa to 0.021 MPa. Moreover, it can be found even though the addition of the commercial stabilizer could enhance the tensile strength of the stabilized soil, the tensile strengths of the CE treated soil and the CE-C treated soil become very similar after soaking.

(4) Figure 5.6 shows the test results of water soaked CE3.5-C0.1 sample with a curing age of 7 days, 14 days or 28 days. The improvement of splitting tensile strength indicates a linear relationship between the curing age and the strength. The effect of commercial stabilizer on the splitting tensile strength for a long period needs further investigations. .

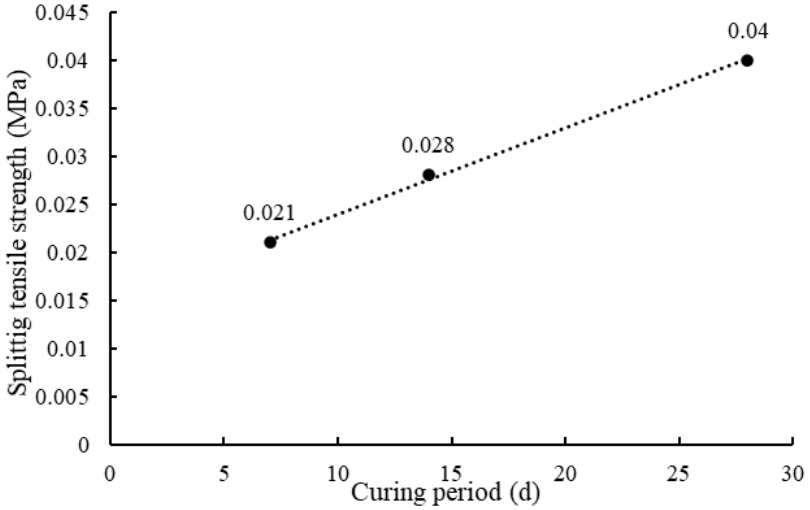

Figure 5.6 Splitting tensile strengths of water soaked CE3.5-C0.1 sample

5.4 Effect of the pre-curing age before compaction

This part of study was investigated by unconfined compression tests. The fine grain soil has been selected for this part of study. The common engineering stabilizers – cement, fly ash and lime had been used to stabilize the soil samples. The moisture content was fixed at 20%. As the pre-curing age before compaction was considered, some of the stabilized soil were mixed and precured for a period of 1, 3 or 7 hours. The samples after compaction are cured for another 7 days under a same condition. Table 5.4 shows all the cases considered and Figure 5.7 shows the variation trend of the strength with the varying pre-curing ages.

Table 5.4 Test plan and UCS results for pre-curing age

Sample	CaO (%)	Fly ash (%)	Cement (%)	Pre-curing time (h)	UCS (MPa)
CA2-FA4-M20-T7	2	4	0	0	0.186
CA2-FA4-M20-T7-R1	2	4	0	1	0.137
CA2-FA4-M20-T7-R3	2	4	0	3	0.121

CA2-FA4-M20-T7-R5	2	4	0	5	0.126
CA2-FA4-M20-T7-R7	2	4	0	7	0.109
CA2-FA4-CE2-M20-T7	2	4	2	0	0.326
CA2-FA4-CE2-M20-T7-R1	2	4	2	1	0.287
CA2-FA4-CE2-M20-T7-R3	2	4	2	3	0.267
CA2-FA4-CE2-M20-T7-R5	2	4	2	5	0.282
CA2-FA4-CE2-M20-T7-R7	2	4	2	7	0.274

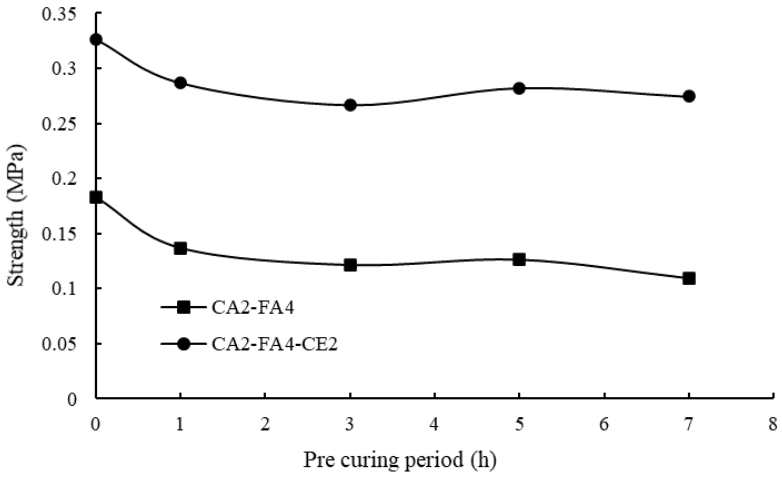

Figure 5.7 Influence of pre-curing age on UCS of fine grain soil

Figure 5.7 shows the UCSs with cement are obviously higher than those without cement. However, whether or not cement is added, the influence of pre-curing age on the unconfined compressive strength of stabilized soil shows similar changing tendencies. The 7-day UCS could be maximized without pre-curing age. This could be because the compaction destroys the cementitious structure formed during the pre-curing process. Meanwhile, it is worth noting that as the strength of stabilized soil generally increases with the increase of dry density, the addition of stabilizers, especially lime, decreases the moisture content of stabilized soil, making it closer to the optimal moisture content, and therefore increase the UCS. But this effect will be weakened after most of the quick lime has been reacted with water., accompanying with an increasing possibility of the strength loss under compaction. In practice, workability of the stabilized soil should also be considered. It has been found that after a 3-hours precuring, the mixture became too hard to be compacted, i.e. lower workability. Therefore, in practice, construction is suggested finishing within 3 hours.

5.5 Effect of stabilizer addition order

The fine grain soil had been selected for this part of study. Table 5.5 shows the test plan and results. Two stabilizer addition orders were considered. For the first type, the soil and the cement was mixed first, followed by adding water. Then, the sample was left for pre-cured for a certain time before compaction . For the second type, the soil with quick lime and fly ash was mixed with water first, followed by adding cement after a certain time of pre-curing. The postfix of T in Table 5.5 indicate the second type of addition order. Different pre-curing times,1 hour, 3 hours, 5 hours and 7 hours were also considered.

Table 5.5 Test plan and UCS results for stabilizer addition order

Sample	CaO (%)	Fly ash (%)	Cement (%)	Pre-curing time (h)	UCS (MPa)
CA2-FA4-CE2-M20-T7-R1	2	4	2	1	0.287
CA2-FA4-CE2-M20-T7-R3	2	4	2	3	0.2669
CA2-FA4-CE2-M20-T7-R5	2	4	2	5	0.282
CA2-FA4-CE2-M20-T7-R7	2	4	2	7	0.274
CA2-FA4-CE2-M20-T7-R1-L	2	4	2	1	0.260
CA2-FA4-CE2-M20-T7-R3-L	2	4	2	3	0.284
CA2-FA4-CE2-M20-T7-R5-L	2	4	2	5	0.303
CA2-FA4-CE2-M20-T7-R7-L	2	4	2	7	0.232

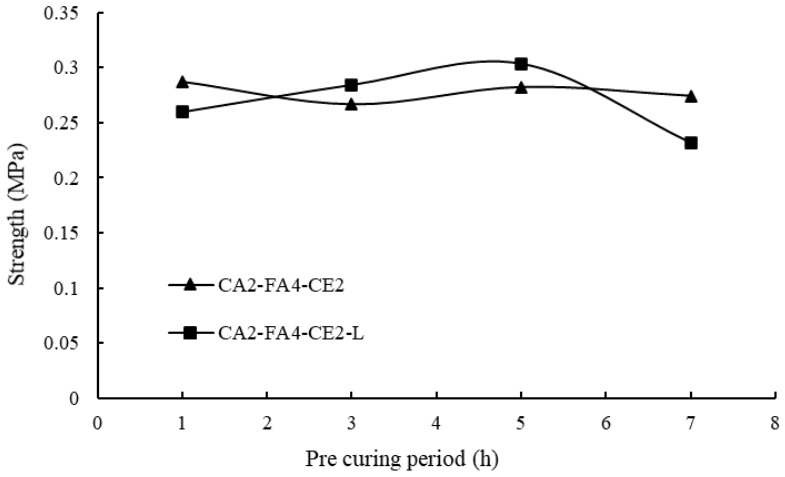

Figure 5.8 Influence of stabilizer addition order on UCS of fine grain soil

The results show that CA2-FA4-CE2-L fluctuates more obviously than CA2-FA2-CE2. In the case of short pre-curing age (such as 1 hour), the strength of stabilized soil obtained by first adding cement is obviously better than that of adding the cement later. This is because the first adding cement can ensure the uniformity of cement dispersion, which is conducive to the formation of an overall strength. With the increase of pre-curing age, such as 3 or 5 hours, the stabilized soil strength of the later adding cement is better than that of the first adding cement. This could be because the pozzolanic reaction of cement is the main strength source of the strength, adding water first makes the quick lime reacts with water. The formation of $Ca(OH)_2$ provides a more favorable reaction condition for the pozzolanic reaction of cement. The pozzolanic reaction stage of cement is relatively early, and the strength of stabilized soil is obviously enhanced. However, with the increasing of pre-curing time, most of the water will be consumed by the quick lime and the remaining water content may not enough for the following pozzolanic reaction. This makes the strength of CA2-FA4-CE2-L becomes smaller than that of CA2-FA4-CE2.

5.6 Summary

The experimental results show that the strength of stabilized soil would be increased with the increase of curing age. For both cement stabilized soil and cement-commercial stabilizer stabilized soil, the strengths (unconfined compressive strength and splitting tensile strength) show approximate linear relationships with the curing ages. The reaction between the cement and the soil is relatively quick and drastic, which can provide the early strength for the stabilized soil , while, for stabilizers such as fly ash, the pozzolanic reactions are slow. So the strength would still increase after 28 days. For such cases, properties of the stabilize soil after 28-day curing needs further studies.

From the triaxial shear test results, it can be found that the addition of commercial stabilizer would lead to a decrease of the cohesion, whereas an increase of the internal friction angle. The curing age has a significant effect on the cohesion. The cohesion would increase greatly when the curing age increases from 7 days to 28 days. In addition, the increase of the curing age would lead to the increase of the peak axial stress, the failure mode of sample would

transfer from drum shaped failure to brittle failure gradually with an increasing addition of the stabilizer.

From the splitting tension test results, some conclusions can be obtained. For cement stabilized samples, the effect of water soaking on the splitting tensile strength is obvious. And for sample stabilized by both cement and commercial stabilizer, it could be found that commercial stabilizer has a positive effect on improving the splitting tensile strength of stabilized soil without soaking, but the effect of water soaking becomes more obvious. The results demonstrate that the samples after 7 days curing do not show good water resistance properties, but the water resistance properties for the samples cured by a longer time need further studies.

The precuring treatment also has effect on the strength of the stabilized soil but not very significant. Considering the workability, construction is suggested finishing in 3 hours if cement is used. The suggested construction time could be extended to some extend due to the use of stabilizes with lower reaction rates.

In terms of the mix order, its effect on the strength of stabilized soil is related to the pre-curing period. There exist an optimum pre-curing time which can maximize the UCS of stabilized soil when the cement is mixed after pre-curing.

The following practical suggestions can be proposed as below:

(1) It is recommended to carry out the construction immediately after soil and stabilizers are mixed.

(2) If the construction cannot be carried out immediately due to the space and time constraints, it is suggested completing the construction within 3 hours.

(3) When stabilizer with relatively slower reaction rate (such as lime, fly ash, etc.), the completion of the construction within 1 to 7 hours would not have a significant effect on the strength of the stabilized soil.

(4) The construction method of adding cement later can be considered as an efficient manner to improve the strength of the stabilized soil when the optimum precuring time is known,

Chapter 6: Effect of wetting-drying cycle on the UCS of stabilized soil

6.1 Introduction

In this chapter, the influence of wetting-drying cycle (W-C cycle) on the unconfined compressive strength of the stabilized soil is investigated. In particular, the effects of the number of wetting-drying cycles, the curing time and the initial moisture content are discussed in detail. Dewatered drilling slurry - B is selected for this part of study.

6.2 Test plan and test procedure

In this study, each wetting-drying cycle was divided into a drying part and a wetting part. For the drying part of the cycle, the stabilized soil sample after curing age was immersed into water for 24 hours. And for the drying part, the stabilized soil sample after wetting was put into an oven with a constant temperature of 40 ℃ for another 24 hours. The procedure of sample preparation were the same as the procedure of the unconfined compression test. Only cement was applied for this part of study as the stabilizer.

The samples had three different curing ages of 7, 14 and 28 days. And the number of the wetting-drying cycles were selected as 0, 1, 2 and 3. The moisture contents of these samples were varied from 20% to 26%. Table 6.1 and Table 6.2 show the samples produced for this part of study. The samples could be divided into two parts. The first part is the samples stabilized with 3.5% cement. These samples have the moisture contents of all the 20%, 22%, 24% and 26%. And the curing ages for these samples is 7 days, 14 days and 28 days. This part aims to investigate the effect of moisture content and curing age on the strength of stabilized soil under the wetting-drying cycle condition. The second part has two types of samples. The first one is the sample stabilized by 4% cement with a moisture content of 22%. The other one type is the sample stabilized by 6.5% cement with a moisture content of 24%. These two types of sample have the same strength values when the curing age are 7 days. The object of this group is to investigate the influence of wetting-drying cycle on the stabilization effect of

cement during a relatively long period (from 7 days to 28 days).

Table 6.1 Test plan and results for Group 1

Samples name	Cement content (%)	Moisture content (%)	Curing age (d)	Cycle times	UCS (MPa)
CE3.5-M20-T7	3.5	20	7	0	0.588
55CE3.5-M20-T7-WD1	3.5	20	7	1	1.577
CE3.5-M20-T7-WD2	3.5	20	7	2	1.776
CE3.5-M20-T7-WD3	3.5	20	7	3	1.597
CE3.5-M22-T7	3.5	22	7	0	0.403
CE3.5-M22-T7-WD1	3.5	22	7	1	0.950
CE3.5-M22-T7-WD2	3.5	22	7	2	0.864
CE3.5-M22-T7-WD3	3.5	22	7	3	0.770
CE3.5-M24-T7	3.5	24	7	0	0.248
CE3.5-M24-T7-WD1	3.5	24	7	1	0.673
CE3.5-M24-T7-WD2	3.5	24	7	2	0.772
CE3.5-M24-T7-WD3	3.5	24	7	3	0.563
CE3.5-M26-T7	3.5	26	7	0	0.215
CE3.5-M26-T7-WD1	3.5	26	7	1	0.600
CE3.5-M26-T7-WD2	3.5	26	7	2	0.503
CE3.5-M26-T7-WD3	3.5	26	7	3	0.325
CE3.5-M20-T14	3.5	20	14	0	0.620
CE3.5-M20-T14-WD1	3.5	20	14	1	1.613
CE3.5-M20-T14-WD2	3.5	20	14	2	2.040
CE3.5-M20-T14-WD3	3.5	20	14	3	1.967
CE3.5-M22-T14	3.5	22	14	0	0.459
CE3.5-M22-T14-WD1	3.5	22	14	1	1.467
CE3.5-M22-T14-WD2	3.5	22	14	2	1.951
CE3.5-M22-T14-WD3	3.5	22	14	3	1.806
CE3.5-M24-T14	3.5	24	14	0	0.320
CE3.5-M24-T14-WD1	3.5	24	14	1	0.812
CE3.5-M24-T14-WD2	3.5	24	14	2	0.912
CE3.5-M24-T14-WD3	3.5	24	14	3	0.757
CE3.5-M26-T14	3.5	26	14	0	0.280
CE3.5-M26-T14-WD1	3.5	26	14	1	0.622
CE3.5-M26-T14-WD2	3.5	26	14	2	0.534
CE3.5-M26-T14-WD3	3.5	26	14	3	0.394
CE3.5-M20-T28	3.5	20	28	0	0.676
CE3.5-M20-T28-WD1	3.5	20	28	1	1.790
CE3.5-M20-T28-WD2	3.5	20	28	2	1.935

CE3.5-M20-T28-WD3	3.5	20	28	3	1.899
CE3.5-M22-T28	3.5	22	28	0	0.547
CE3.5-M22-T28-WD1	3.5	22	28	1	1.468
CE3.5-M22-T28-WD2	3.5	22	28	2	1.849
CE3.5-M22-T28-WD3	3.5	22	28	3	1.450
CE3.5-M24-T28	3.5	24	28	0	0.384
CE3.5-M24-T28-WD1	3.5	24	28	1	0.807
CE3.5-M24-T28-WD2	3.5	24	28	2	1.029
CE3.5-M24-T28-WD3	3.5	24	28	3	0.815
CE3.5-M26-T28	3.5	26	28	0	0.355
CE3.5-M26-T28-WD1	3.5	26	28	1	0.772
CE3.5-M26-T28-WD2	3.5	26	28	2	0.612
CE3.5-M26-T28-WD3	3.5	26	28	3	0.538

Table 6.2 Test plan and results for Group 2

Samples name	Cement content (%)	Moisture content (%)	Curing age (d)	Cycle times	UCS (MPa)
CE4-M22-T7	4	22	7	0	0.424
CE4-M22-T7-WD1	4	22	7	1	1.172
CE4-M22-T7-WD2	4	22	7	2	1.237
CE4-M22-T7-WD3	4	22	7	3	0.914
CE4-M22-T14	4	22	14	0	0.434
CE4-M22-T14-WD1	4	22	14	1	1.224
CE4-M22-T14-WD2	4	22	14	2	1.270
CE4-M22-T14-WD3	4	22	14	3	1.206
CE4-M22-T28	4	22	28	0	0.487
CE4-M22-T28-WD1	4	22	28	1	1.322
CE4-M22-T28-WD2	4	22	28	2	1.609
CE4-M22-T28-WD3	4	22	28	3	1.527
CE6.5-M24-T7	6.5	24	7	0	0.421
CE6.5-M24-T7-WD1	6.5	24	7	1	1.221
CE6.5-M24-T7-WD2	6.5	24	7	2	1.391
CE6.5-M24-T7-WD3	6.5	24	7	3	1.170
CE6.5-M24-T14	6.5	24	14	0	0.457
CE6.5-M24-T14-WD1	6.5	24	14	1	1.357
CE6.5-M24-T14-WD2	6.5	24	14	2	1.454
CE6.5-M24-T14-WD3	6.5	24	14	3	1.260
CE6.5-M24-T28	6.5	24	28	0	0.517
CE6.5-M24-T28-WD1	6.5	24	28	1	1.366
CE6.5-M24-T28-WD2	6.5	24	28	2	1.530
CE6.5-M24-T28-WD3	6.5	24	28	3	1.288

6.3 Results and discussion for Group 1

Experimental results of the Group 1 was summarized in Table 6.1. Figure 6.1 shows the test results of CE3.5 samples (the first part) under different W-D cycles. It is obviously that the samples without W-D cycle had a much lower strength than the samples after different W-D cycles, especially for samples with a relatively low moisture content (20%~24%). For samples with a moisture content 26%, the samples were damaged more severely. Hence the strength of sample after different W-D cycles would decrease because of the damage of sample's structure. For cases with a moisture content of 20%, 22% or 24%, the samples after two W-D cycles had the highest unconfined compressive strengths. The changes of the strength might be due to a combined effect of the water-induced internal structure damage and the curing-induced strength improvement. Sample damaged gradually with the increase of the number of W-D cycle, which leads to a decrease of strength. Meanwhile, with a longer curing age, the strength of samples should have been increasing due to chemical reactions.

For sample with a moisture content of 26%, the moisture susceptibility was higher than samples with lower moisture contents, so that the samples were damaged more severely. Hence, from one W-D cycle to three W-D cycles, the strength of samples decreased. The changes of strength might mainly be caused by the changes of the internal structure of the stabilized soil samples during the W-D cycles. According to the research conducted by Wang et al. (2017), because of the W-D cycle, the spacing within the needle-like network structure becomes larger than same stabilized samples without W-D cycles. The absorption and loss of water alternate inside the samples, and some of the stabilizer components would lose with the loss of water. And cracks of framework structure formed by hydration products would appear and continue to expand. At the end, the loss of stabilizer components and structure cracks would lead to the decrease of unconfined compressive strength. Furthermore, after the W-D cycles, the hydrates of the original stabilizer components precipitate with water loss after the sample experienced W-D cycles, which leads to the destruction of the original hydrates network-like interconnected structure, and makes the pores of the hydrates connected structure become larger, which further weakens the strength of the soil samples. The strength of soil samples also decreased significantly after W-D cycle due to the transformation of the original solid

needle-like network structure of the hydration products of some stabilizers into the more fragile salt-out junction crystal connection structure. Figure 6.2 shows the CE3.5-T14 samples with different moisture contents after different W-D cycles. The samples from left to right are 1 W-D cycle, 2 W-D cycles and 3 W-D cycles, respectively. It is obvious that the damage of sample became more severe from 1 cycle to 3 cycles and from moisture content of 20% to 26%.

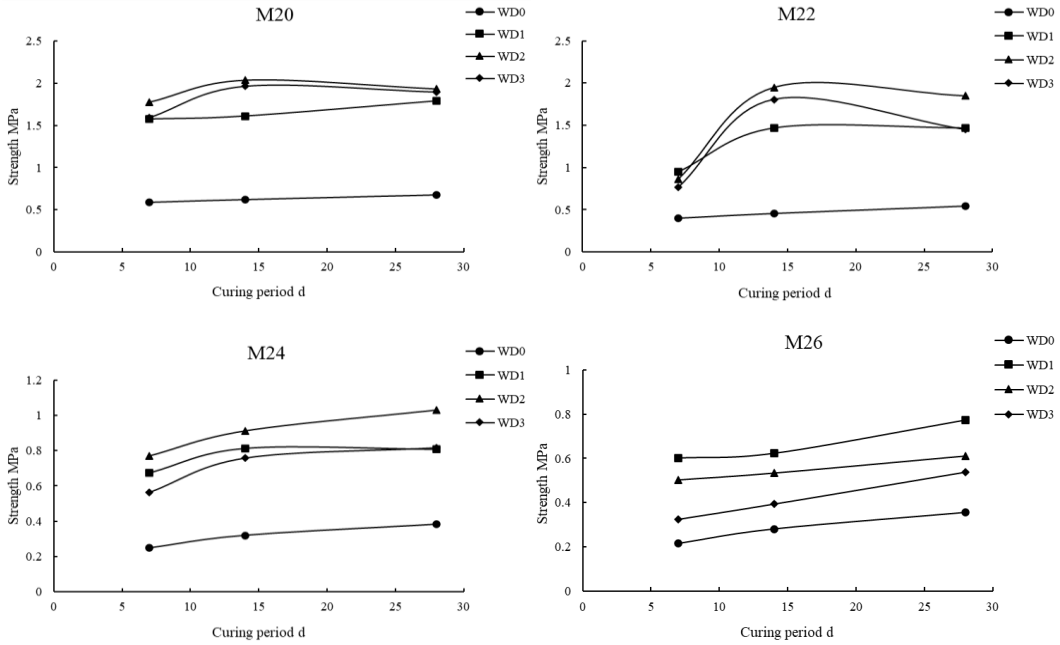

Figure 6.1 Test results of CE3.5 samples under W-D cycles

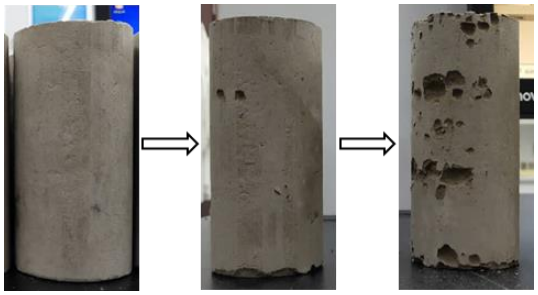

(a) CE3.5-M20-T14

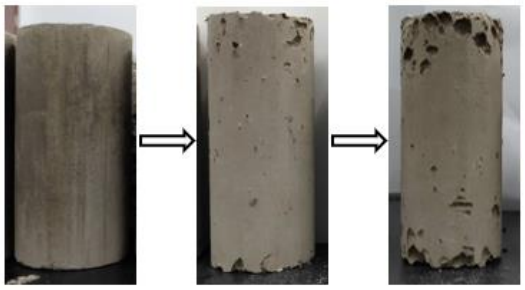

(b) CE3.5-M22-T14

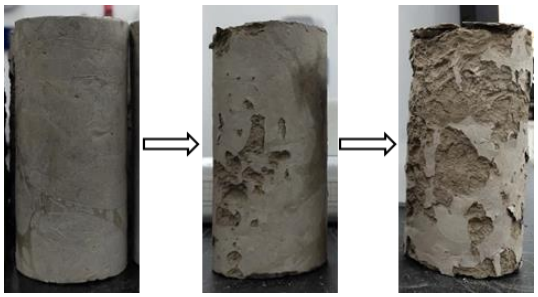

(c) CE3.5-M24-T14

(d) CE3.5-M26-T14

Figure 6.2 CE3.5-T14 samples after different W-D cycles

In addition, the unconfined compressive strength results also show that sample with no W-D cycle had much lower strength than sample with different W-D cycle. To verify this finding and to investigate the effect of wetting and drying on the strength of stabilized soil, three control groups of samples had been prepared as shown in Table 6.3. As can be seen, after 1-day water soaking, the strength of sample decreased from 0.588 MPa to 0.535 MPa with a difference of 9%. After 1-day drying in the oven at a constant temperature of 40℃, the strength of the sample increased to 1.644 MPa with a difference of 179.6%. In addition, another group was prepared without curing age, the strength increased to 2.517 MPa after 7-day drying in the oven, the increasing amplitude was 328.1%. Figure 6.3 further shows the stress-strain relationships for three groups of samples. These curves indicate that water soaking sample

would have a larger failure strain but a lower peak stress value. With a longer period of drying, the sample would have a higher strength but a lower failure strain. In other words, the sample would become more brittle during the drying process. The results agree with the conclusion drawn by Shabjareh et al. (2014) that samples' brittleness is increased as the number of W-D cycles increases. They also found that a higher temperature (from 23 ℃ to 65 ℃) would increase the brittleness of samples.

Table 6.3 Test results for control groups

Sample	Curing age (d)	Water soaking (d)	Drying (d)	UCS (MPa)
CE3.5-M20-T6-W1	6	1	0	0.535
CE3.5-M20-T6-D1	6	0	1	1.644
CE3.5-M20-D7	0	0	7	2.517

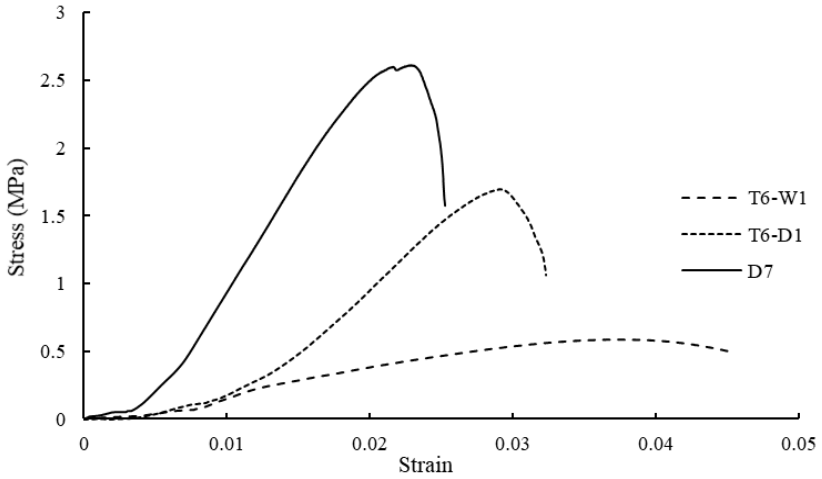

Figure 6.3 Stress-strain relationships for control groups

6.4 Results and discussion for Group 2

Figure 6.4 shows the UCS results for Group 2 samples. It can be found from the three figures that the two groups of samples had similar strength with no W-D cycle. Then the strength differences would become larger with the processing of W-D cycles, and CE6.5-W24 samples always have larger strength than CE4-W22 samples. This result also show that the effect of increasing 2.5% cement on strength and moisture susceptibility exceeds that of decreasing 2% moisture content. The samples with a higher cement content (6.5%) have a lower moisture

susceptibility. Figure 6.5 shows the changes of these two groups of samples after different W-D cycles. It can be seen that the CE4-W22-T14 samples were more damaged by several W-D cycles than the CE6.5-W24-T14 samples.

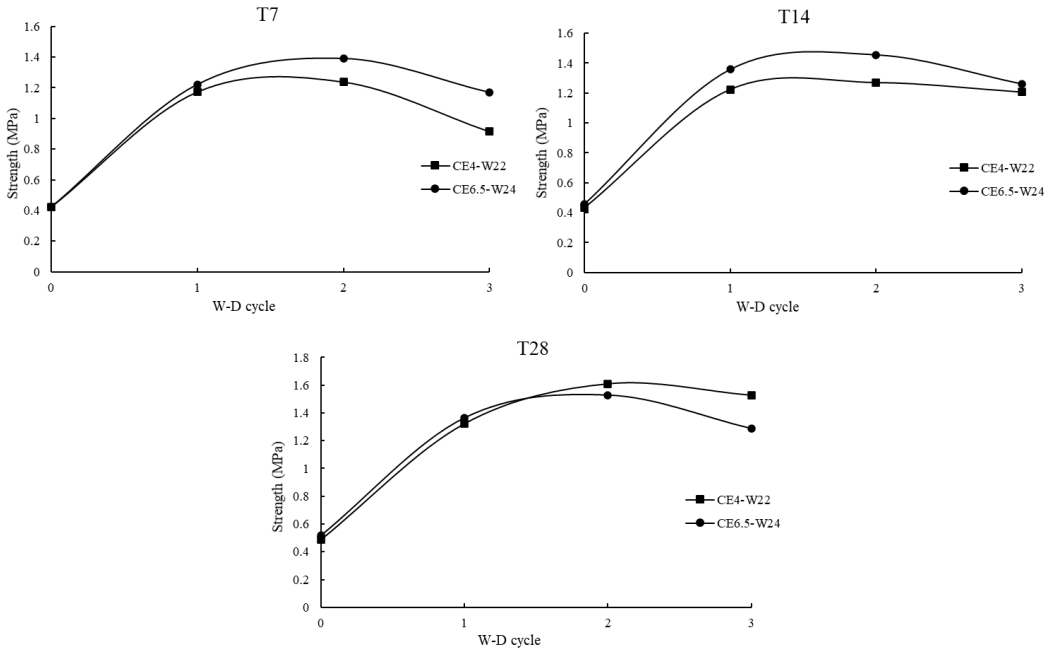

Figure 6.4 Test results of CE4-W22 and CE6.5-W24 samples

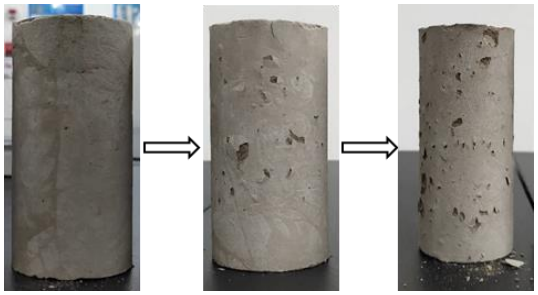

(a) CE4-M22-T14

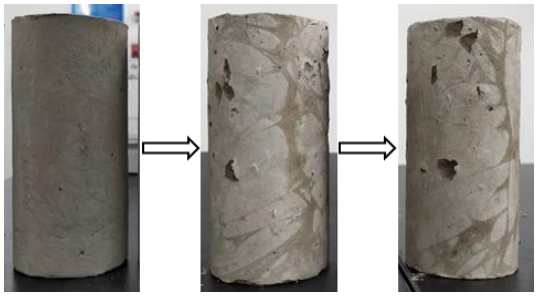

(b) CE6.5-M24-T14

Figure 6.5 Samples after W-D cycles

6.5 Summary

The samples without W-D cycle had much lower strengths than the samples after different W-D cycles because the high temperature (40 ℃) curing process would promote the stabilization reactions between cement and soil. Moreover, the strength of samples after W-D cycles increased from 1 cycle to 2 cycles and then decreased when the cycle number increased to 3. The variations of strength might be caused by the combined effects of water-induced structure damage and curing-induced strength improvement. With a larger cement content, the resistance of the stabilized soil to the W-D cycle would be stronger because of its lower water susceptibility.

Chapter 7: Numerical analysis

The numerical analysis part was conducted to simulate the behavior of pavement structure and subgrade after construction and under traffic loads. Settlement and stability of the stabilized pavement subgrade will be evaluated. The static load on the pavement was estimated based on the data in Qiu and Yu (2010), considering a 20ton truck moving on the pavement surface at a speed of 60 km/h.

7.1 Finite element model

The finite element simulations were conducted using the commercial software ABAQUS. The two-dimensional finite element model in Figure 7.1 shows an asphaltic pavement structure and an embankment subgrade laying on a soft subsoil.

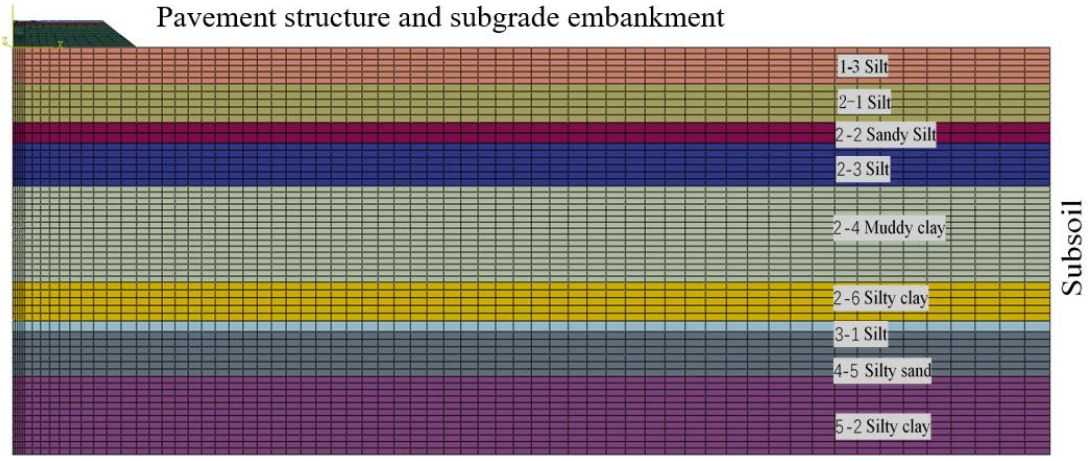

Figure 7.1 Finite element model for the pavement laying on a soft soil

To save the computational effort, only half model was considered with a symmetric boundary condition applied on the left side of the model. A pore pressure boundary condition was applied on the top of the subsoil to allow the water passing through during a consolidation process. The bottom of the model was constrained in the vertical direction and the right side of the model was constrained in the horizontal direction. The geometry and material properties are given in the next section. In total 16 CPE8R (4-node bilinear plane strain quadrilateral,

reduced integration, hourglass control) elements were used in the pavement structure and 5330 CPE8RP (8-node plane strain quadrilateral, biquadratic displacement, bilinear pore pressure, reduced integration) elements were applied in the subsoil. Three traffic lines with a width of 3.75m for each were considered for the half model. The traffic load was uniformly distributed in these three lines and magnitude of the vertical stress is 50kPa.

During the simulation, a geostatic step is first applied to ensure equilibrium. Then, the embankment subgrade, comprising of 11 layers of stabilized soil, was added layer by layer to simulate a multi-stage construction of the subgrade. After that, the pavement structure and the traffic load was applied, and a consolidation stage was applied over a long period to assess its final settlement.

7.2 Layer thickness and material properties

For the pavement structure, layer thickness and the material properties in each layer are summarized in Table 7.4. The materials of the pavement structure is assumed to be elastic. The stabilized soil and the granular soil were assumed to follow Mohr-Coulomb yield criterion. Mohr-Coulomb parameters were determined in Chapter 5 considering three different curing ages.

In term of the subsoil, the constitution and material properties of the subsoil are obtained from a ground investigation report for an express way in Ningbo, listed in Table 7.5. Materials in Layer 5,6 and 9 were considered as elastic plastic strain hardening materials described by a modified Cam-clay plasticity model. The other materials followed Mohr-Coulomb yield criterion. The Mohr-Coulomb parameters were determined through direct shear test, whereas the Cam-clay model parameters were obtained based on the calculation process given below.

In ABAQUS, the following equation has been used to describe this model:

$$\frac{1}{\beta^2}\left(\frac{p}{a}-1\right)^2+\left(\frac{t}{Ma}\right)^2-1=0$$

Equation 7.1 Yield surface function

In the Equation 7.1, M is the slope of the critical state line CSL on the p-q plane; a is the

size of p corresponding to the intersection of the yield trajectory and the critical state line; β is the parameter that controls the shape of the yield surface.

When using the Cam-clay model in ABAQUS, the model parameters include the slope of the critical state line M, the slope of isotropic consolidation line λ, the slope of unloading-reloading line κ, Poisson's ratio μ, parameter reflecting the size of the initial yield surface a_0, parameter that control the shape of the yield surface β and the yield stress ratio between triaxial tension and triaxial compression K and other parameters. To modify the seepage coupling model of the Cam-clay model and Biot consolidation theory coupling, it is also necessary to add the permeability coefficient k.

(1) Slope of the critical state line M

Cam-clay model is an ellipsoid in the three-dimensional stress state, that is, the yield locus on the π plane is a circle. According to the failure conditions determined by the triaxial conventional compression, the following equation can be obtained as:

$$M = (6\sin\varphi) / (3-\sin\varphi)$$

φ indicates the internal friction angle

Equation 7.2 Calculation of M

(2) Slope of isotropic consolidation line λ

Previously, many scholars have studied the correlation between soil parameters and plasticity index I_P. Mayne (2001) made a more comprehensive prediction of the relationship between Cam-clay model parameters and plasticity index I_P; Ishii et al. (1955) proposed that there is a linear relationship between I_P and the compressibility of soil; Chen et al. (2003) summarized the geotechnical survey test data in the Shanghai area, and obtained the relationship between the isotropic consolidation parameter λ and plasticity index I_P in the revised Cam-clay model is:

$$\lambda = 0.0165 I_P - 0.01309$$

Equation 7.3 Calculation of λ

In view of the fact that the situation of Ningbo soft soil is relatively close to that of Shanghai soft soil, the Equation 3.3 can be sued to calculate the slope of isotropic consolidation curve λ.

(3) Slope of unloading-reloading line κ

Chen et al. (2003) conducted regression statistics on the slope of unloading-reloading line κ and plasticity index I_P and found that the relationship between the two parameters is:

$$\kappa = 0.0036\, I_P - 0.0336$$

Equation 7.4 Calculation of κ

Normally, the plasticity index of the soil layer close to the surface is small. When $I_P < 5$, the equation above will have $\kappa < 0$. At this time, the recommended value can be considered to determine the value of the slope of unloading-reloading line κ, see Table 7.1.

Table 7.1 Recommended value of unloading-reloading parameter κ for some soil layers in Ningbo soft soil area

Soil layer	Silty clay	Mucky soil	Clay
κ	0.018	0.025	0.022

(4) Poisson's ratio μ

Poisson's ratio is the ratio of the lateral strain to the vertical strain of the soil. According to the generalized Hooke's law of material mechanics, the relationship between Poisson's ratio and lateral pressure coefficient K_0 can be derived as below:

$$\mu = K_0 / (1 + K_0)$$

Equation 7.5 Calculation of μ

The lateral pressure coefficient K_0 can be obtained from the geotechnical engineering survey report. Generally, μ = 0.3 – 0.35 for sandy soil, μ = 0.35 – 0.4 for silty soil, μ = 0.4 – 0.45 for silty clay, and μ = 0.45 -0.5 for clay.

(5) Parameter reflecting the size of the initial yield surface a_0

a_0 reflects the size of the initial yield surface, it can be calculated by equation below according to initial stress and void ratio:

$$a_0 = 0.5 \exp((e_1 - e_0 - \kappa \ln p_0) / (\lambda - \kappa))$$

Equation 7.6 Calculation of a_0

In the equation, e_0 is the initial void ratio, e_1 is the void ratio at lnp=0 on the v-lnp curve. In ABAQUS, the value of e_1 can be entered directly in the input box, and then the software can calculate the value of a_0 according to the theoretical equation. At this time, there is no need to set a_0 in the Data list.

(6) Parameter that control the shape of the yield surface β

β is a constant representing the yield of the yield surface cap. As shown in Figure 7.1, when on the side of q > Mp, β = 1; when on the side of q < Mp, β may not be equal to 1, affecting the shape of yield surface on this side. When the value of β is smaller, the yield surface is tighter, the soil state is wetter, and its compressibility is greater. The recommended values of β for same soil layers have been shown in Table 7.2.

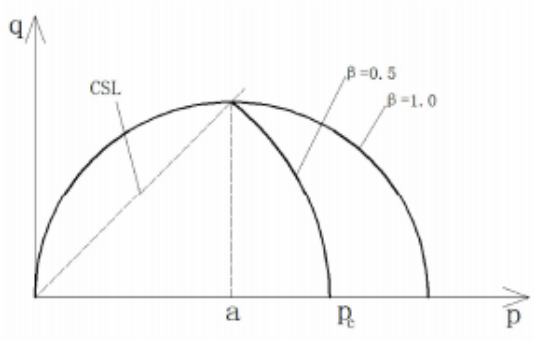

Figure 7.2 Yield surface for Cam-clay model

Table 7.2 Recommended value of β for same soil layers in Ningbo soft soil area

Soil layer	Silty clay	Mucky soil	Clay
β	1	0.85	0.9

(7) Yield stress ratio between triaxial tension and triaxial compression K

K is the yield stress ratio between triaxial tension and triaxial compression, it is used to control the shape of the yield surface on the π plane. At present, there is little research on K value at home and abroad, and there is no corresponding empirical equation. Li et al. (2010) compared the results of the simulation calculation with the measured values and concluded that the yield stress ratio K has a very small effect on the settlement calculation results, K can be ignored in the calculation. The recommended values of K for some soil layers have been shown in Table 7.3.

Table 7.3 Recommended value of K for same soil layers in Ningbo soft soil area

Soil layer	Silty clay	Mucky soil	Clay
K	0.87	0.89	0.84

Seepage flow was considered for all the subsoil layers by defining vertical seepage flow coefficient k_v and horizontal seepage flow coefficient k_h in ABAQUS. All the related parameters are summarized in Table 7.6.

Table 7.4 Layer thickness and material parameters for the pavement structure

	Material	Thickness (mm)	Stiffness modulus (MPa)	Poisson's ratio	Density (g/cm^3)	C (kPa)	ϕ (°)	ψ (°)
1	SMA-13	40	1991	0.35	2.5	/	/	/
2	Sup-20	60	1425	0.35	2.5	/	/	/
3	Sup-25	100	978	0.35	2.5	/	/	/
4	Cement macadam	200	3188	0.25	2.4	/	/	/
5	Cement macadam	360	2167	0.25	2.4	/	/	/
6	Stabilized soil	340	44.5 (28 days) 29.5 (14 days) 25.1 (7 days)	0.25	1.9	224 (28 days) 150 (14 days) 135 (7 days)	26.5 (28 days) 26 (14 days) 22.5 (7 days)	0
7		300						
8		300						
9		300						
10		300						
11		300						
12		300						
13		300						
14		300						
15		300						
16		300						
17	Granular soil	300	150	0.2	2.8	45	10	10

Table 7.5 Layer thickness and material properties in each layer of the subsoil

Layer	Label	layer thickness（m）	material	initial moisture content w (%)	density ρ (g/cm^3)	Gravity G_s	void ratio e	Saturability S_r (%)	Liquid limit (%)	Plastic limit (%)	plastic index I_P	liquid index I_L
1	①3	6	Silt	28	1.91	2.7	0.814	93	28.4	19	9.4	1.1
2	②1	6.42	Silt	26.4	1.9	2.7	0.797	89.7	29.3	20.7	8.6	0.92
3	②2	3.4	Silty sand	21.4	1.98	2.69	0.654	88.2	28.5	19.1	9.4	0.24
4	②3	7.1	Silt	29.3	1.88	2.7	0.882	91.8	31.8	22.5	9.3	1.22
5	②4	15.9	Muddy clay	44	1.75	2.74	1.27	98.4	43.5	23.7	19.7	1.08
6	②6	6.4	Silty clay	34.9	1.83	2.72	1.014	93.5	38	20.8	15.4	0.94
7	③1	1.8	Silt	26	1.91	2.7	0.787	89.4	27.7	18.7	9	0.92
8	④5	7.4	Silty sand	21.4	1.98	2.69	0.654	88.2	28.5	19.1	9.4	0.24
9	⑤2	12.9	Silty clay	38.2	1.81	2.74	1.091	95.7	47.5	25.4	22.2	0.58

Table 7.6 Property parameters of the subsoil

x	Label	Seepage flow coefficient		Mohr Coulomb parameters		Modified cam-clay parameters					
		k_h (m/day)	k_v (m/day)	c (kPa)	f（°）	M	λ	κ	μ	β	K
1	①3	0.05	0.05	14.0	27.6	/	/	/	/	/	/
2	②1	0.05	0.05	10.5	30.5	/	/	/	/	/	/
3	②2	0.05	0.05	8.8	29.8	/	/	/	/	/	/
4	②3	0.00	0.00	10.8	29.3	/	/	/	/	/	/
5	②4	0.00	0.00	/	/	0.47	0.19	0.04	0.40	0.85	0.89
6	②6	0.05	0.05	/	/	0.63	0.12	0.02	0.37	1.00	0.89
7	③1	0.52	0.52	10.0	30.0	/	/	/	/	/	/
8	④5	1.04	1.04	8.8	29.8	/	/	/	/	/	/
9	⑤2	0.00	0.00	/	/	0.68	0.24	0.05	0.37	1.00	0.84

7.3 Results and analyses

The settlement of the subsoil surface after construction (i.e. pre-loading consolidation) is shown in Figure 7.3. The surface deformations of the subsoil soil under traffic loads are also given considering three different curing ages. Results show that the curing ages do not affect the deformation of subsoil significantly. But the settlement of the subsoil surface increases from 0.225mm to around 0.34mm due to the application of the traffic load. Besides, the analysis also shows the deformation mainly occurs in the soft soil layers ②4 and ②6. Despite of that, since the overall thickness of the layers above the soft soil layers is considerable thick, deep sliding is not possible for the current construction.

Surface deformation of the pavement structure under the traffic load is given in Figure 7.4. Results show that the effect of curing age on the surface deformation is very limited. However, the change of the stabilized soil properties due to different curing ages affect the stress distribution obviously. From Figure 7.5, the maximum tensile stresses in the embankment are at the bottom, and the stress magnitude increases from 11.2 kPa to 80.6 kPa when the curing age increases from 7 days to 28 days. The 7-days tensile strength has been measured to be 106 kPa which is much larger than the maximum tensile stress. Therefore, the embankment should not fail due to the tensile failure of the materials. Besides, no yielding areas have been found in the embankment for all these three cases (as shown in Figure 7.6), which means the shear strength of the stabilized soil is large enough to prevent the embankment from a shear failure.

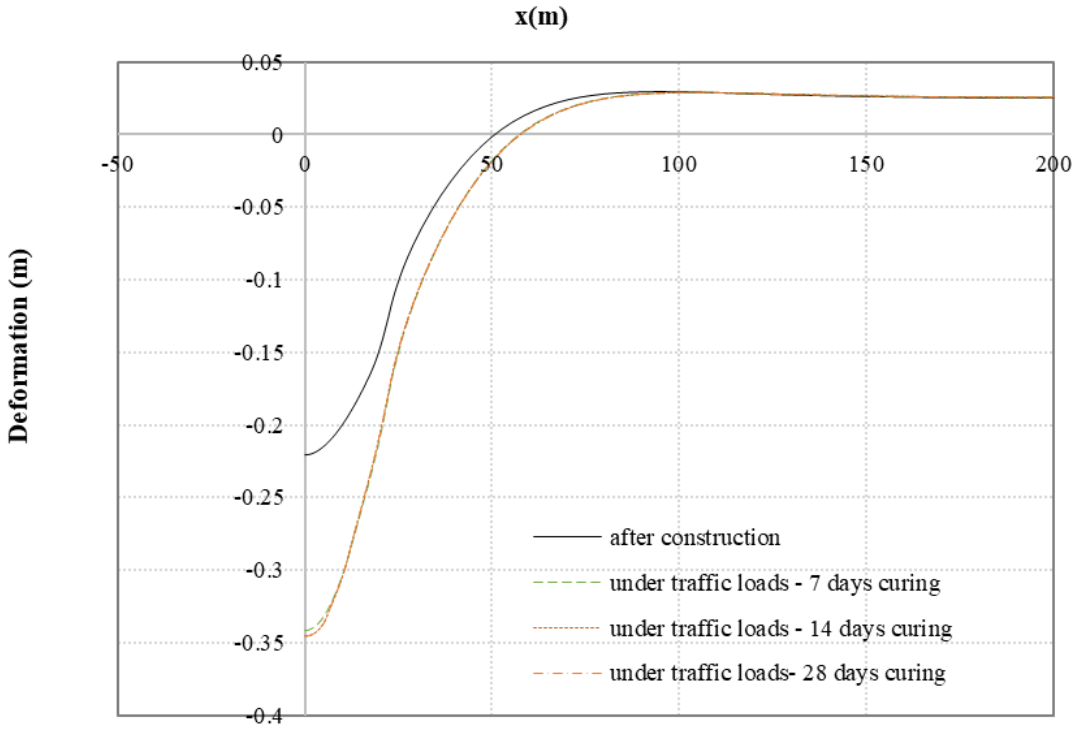

Figure 7.3 Settlement of subsoil after construction and under traffic loads

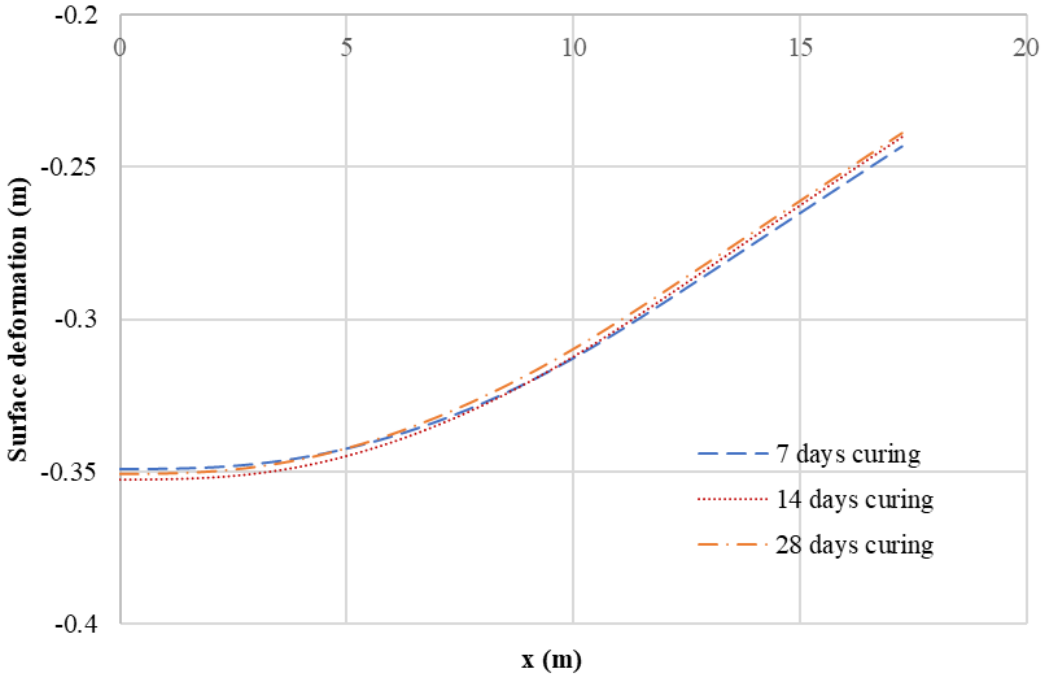

Figure 7.4 Surface deformation of the pavement

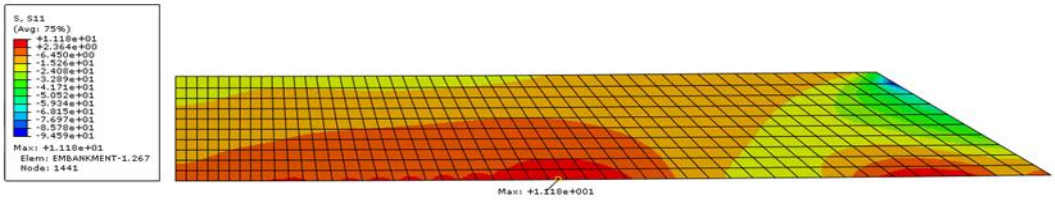

(a) 7 days curing

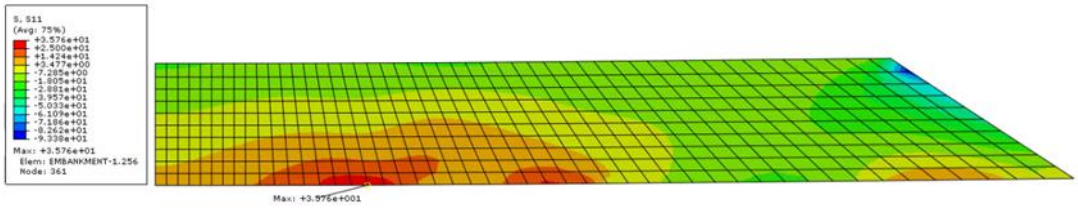

(b) 14 days curing

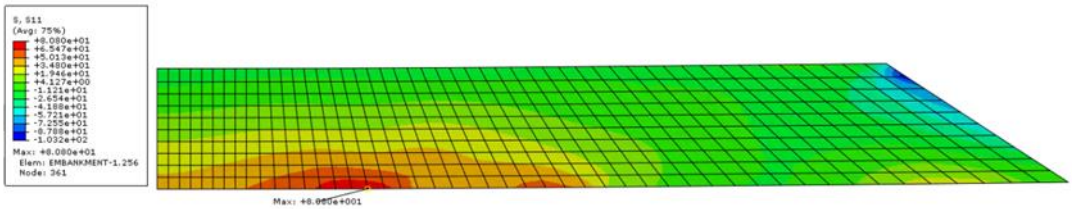

(c) 28 days curing

Figure 7.5 Tensile stress contour for the embankment under the traffic load

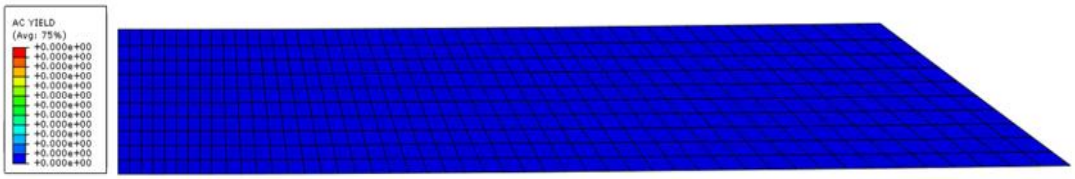

Figure 7.6 Yielding condition of the embankment under the traffic load

Chapter 8: Conclusion and future work

8.1 Conclusion

This study investigated the mechanical properties of stabilized soil by both experimental study and mechanical analysis. The conclusions of this study can be listed as below:

(1) There exists a positive linear relationship between cement content and the unconfined compressive strength. The effect of the cement content on the unconfined compressive strength is higher than gypsum, followed by lime and fly ash. For both fly ash and gypsum, there exist optimum contents that can maximize the unconfined compressive strength. it can be further concluded that cement is the most effective stabilizer for the fine soil. An addition of a proper content of gypsum can further increase the strength.

(2) The stabilized soil is expected to obtain the maximum strength when it was prepared at the optimum moisture content. At the dry-side of the optimum moisture content, the strength would have an increasing trend; at the wet-side of the optimum moisture content, the strength would show a decreasing trend.

(3) An increasing curing age can help the stabilized soil gain more UCS strength as well as cohesion and splitting tensile strength. The stabilized soil sample without a pre-curing before compaction has larger 7-day UCS than the samples pre-cured before compaction. For the samples pre-cured before compaction, there exists an optimum pre-curing time that can maximize the strength of the stabilized soil.

(4) An obvious increase of the UCS of cement stabilized soils has been observed due to the application of one to three W-D cycles, since the stabilization reactions between cement and soil could been promoted. A maximum strength can be observed when 2 W-D cycles were applied, due to the change of moisture content during drying. Further W-D cycles application leads to a decreasing strength, as the internal structure of the stabilized soil has been damaged by the water.

(5) Settlement of the subsoil has been predicted through numerical analyses. The application of traffic load results in a further deformation (from 0.225m to around 0.34m) on the subsoil surface. Stress distribution in the embankment has also be obtained and results show that the strength of the stabilized soil meet the requirements of the pavement to prevent it from both tensile failure and shear failure.

8.2 Future work

(1) Samples strength after a longer curing age needs a further investigation.

(2) More W-D cycles will be considered in the future. The effect of drying temperature will also be investigated.

(3) Reaction mechanism of the commercial stabilizer will be studied in the future. More studies will also be carried out.

Reference list

AHMED, A. & EL NAGGAR, M. H. 2018. Effect of cyclic loading on the compressive strength of soil stabilized with bassanite–tire mixture. *Journal of Material Cycles and Waste Management,* 20(1)**,** 525-532.

ÅHNBERG, H. & HOLM, G. Influence of laboratory procedures on properties of stabilised soil specimens. International Symposium on Deep Mixing and Admixture Stabilization, DM09, Okinawa, May 19-21, 2009, 2009. Port and Airport Research Institute, 1-6.

BAI, C. 2014. *Experimental study on the solidified soil in road base with performance.* Shenyang Jianzhu University.

BAI, Y. 2009. *Study on road performance and filling technology of solidified muddy soil by fly-ash.* Shanghai Jiao Tong University.

BELL, F. 1995. Cement stabilization and clay soils, with examples. *Environmental & Engineering Geoscience,* 1(2)**,** 139-151.

BELL, F. 1996. Lime stabilization of clay minerals and soils. *Engineering geology,* 42(4)**,** 223-237.

BLáHOVá, K., ŠEVELOVá, L. & PILAŘOVá, P. 2013. Influence of water content on the shear strength parameters of clayey soil in relation to stability analysis of a hillside in Brno region. *Acta Universitatis Agriculturae Et Silviculturae Mendelianae Brunensis,* 61(6)**,** 1583-1588.

BSI 1990. BS 1377-2: Methods of Test for Soils for Civil Engineering Purposes–Part 2 Classification tests. British Standards Institution London.

BSI 2015. BS 5930: Code of practice for ground investigations. British Standards Institution London.

CHEGENIZADEH, A. & NIKRAZ, H. CBR test on reinforced clay. Proceedings of the 14th Pan-American Conference on Soil Mechanics and Geotechnical Engineering (PCSMGE), the 64th Canadian Geotechnical Conference (CGC), 2011. Canadian Geotechnical Society.

CHEN, A., ZHANG, J. & LIU, J. 2011. Experiment on unconfined compressive strength of limme improving expansive clay. *Journal of Guilin Univeristy of Technology,* 31(1)**,** 91-95.

CHEN, J., SUN, H., SHI, Z., et al. 2003. Estimation of parameters of modified Cam-clay model coupling Biot theory. *Journal of Tongji University,* 31(5)**,** 544-548.

CHEN, M., YANG, G. & YU, L. 2013. Experimental study on solidification and stabiliization of polluted silt using fly ash ad sodium hydroxide. *Journal of Huazhong Univeristy of Science & Technology (Natural Science Edition),* 41(10)**,** 123-127.

CHEN, Y., HUANG, B. & CHEN, Y. 2005. Deformation and strength of structural soft clay under cyclic loading. *Chinese Journal of Geotechnical Engineering,* 27(9)**,** 1065-1071.

CHENG, F., HUANG, Y., ZHOU, Z., et al. 2017. Undrained triaxial test of saturated laterite under drying-wetting cycle. *Journal of Engineering Geology,* 25(4)**,** 1017-1026.

CHENG, F., LEI, X., MENG, Q., et al. 2015. Experimental Study on the Mechanical Properties of Solidified Dredging Silt of High Moisture Content. *Science Technology and Engineering,* 15(1)**,** 295-299.

CHENG, J., WANG, Y., MIAO, S., et al. 2014. Property study of solidified loess under wet-dry cycles. *Journal of Engineering Geology,* 22(2)**,** 226-232.

CHINA SPECIFICATIONS, J. 2015. D30-2015: Specifications for Design of Highway Subgrades. China Communications Press, Beijing.

CHRISTOPHER, B. R., SCHWARTZ, C. W., BOUDREAUX, R., et al. 2006. Geotechnical aspects of pavements. United States. Federal Highway Administration.

COKCA, E. 2001. Use of class c fly ashes for the stabilizationof an expansive soil. *Journal of Geotechnical and Geoenvironmental Engineering,* 127(7)**,** 568-573.

CONNER, J. R. 1990. Chemical fixation and solidification of hazardous wastes. *VAN NOSTRAND REINHOLD, NEW YORK, NY(USA). 1990.*

DALTON, J. L., GARDNER, K. H., SEAGER, T. P., et al. 2004. Properties of Portland cement made from contaminated sediments. *Resources, conservation and recycling,*

41(3), 227-241.

DE FIGUEIRêDO LOPES LUCENA, L. C., THOMé JUCA, J. F., SOARES, J. B., et al. 2014. Potential uses of sewage sludge in highway construction. *Journal of Materials in Civil Engineering,* 26(9), 04014051.

DENG, J. 1989. Introduction to grey system theory. *The Journal of grey system,* 1(1), 1-24.

DETZNER, H. D., SCHRAMM, W., DöRING, U., et al. 1998. New technology of mechanical treatment of dredged material from Hamburg harbour. *Water science and technology,* 37(6-7), 337-343.

DIGIOIA, A. M. & NUZZO, W. L. 1972. Fly ash as structural fill. *Journal of the Power Division,* 98(1), 77-92.

FENG, P., HAO, L., HUO, C., et al. 2014. Rheological behavior of coal bio-oil slurries. *Energy,* 66(744-749.

FENG, T.-W., LEE, J.-Y. & LEE, Y.-J. 2001. Consolidation behavior of a soft mud treated with small cement content. *Engineering geology,* 59(3-4), 327-335.

FRAAY, A., BIJEN, J. & DE HAAN, Y. 1989. The reaction of fly ash in concrete a critical examination. *Cement and concrete research,* 19(2), 235-246.

GAO, J.-W., YU, H.-M. & LI, K. 2014. Experimental research on unconfined compression strength of loess. *Safety and environmental engineering,* 21(4), 132-137.

GAU, H., HSIEH, C. & LIU, C. 2006. Application of grey correlation method to evaluate potential groundwater recharge sites. *Stochastic environmental research and risk assessment,* 20(6), 407-421.

GUO, Y. 2007. *Study on stabilization of muddy soil and mechanical properties of stabilized soil.* Zhejiang University.

HAMIDI, A. & HOORESFAND, M. 2013. Effect of fiber reinforcement on triaxial shear behavior of cement treated sand. *Geotextiles and Geomembranes,* 36(1-9.

HAUSMANN, M. 1990. *Engineering principles of ground solidification*, McGraw-Hill Book Co., Inc. New York, USA.

HE, Y., ZHANG, X., ZHANG, Y., et al. 2014. Effects of particle characteristics of lightweight aggregate on mechanical properties of lightweight aggregate concrete.

Construction and Building Materials, 72(270-282.

HILT, G. H. & DAVIDSON, D. 1960. Lime fixation in clayey soils. *Highway Research Board Bulletin,* 262).

HUANG, X. & HU, T. 1998. Experimental study on stabilization of soft soil with waste gypsum and cement. *Chinese Journal of Geotechnical Engineering,* 20(5)**,** 72-76.

HUANG, X., XU, S. & NING, J. 2007. Experimental research on stabilized soft soils by alumina bearing modifier. *Chinese Journal of Rock Mechanics and Engineering,* 26(1)**,** 156-161.

INDRARATNA, A., BALASUBRAMANIAN, A. & KHAN, M. 1995. Effect of fly ash with lime and cement on the behavior of a soft clay. *Quarterly Journal of Engineering Geology and Hydrogeology,* 28(2)**,** 131-142.

ISHII, Y., KURATA, S. & FUJISHITA, T. 1955. Researches on the engineering properties of alluvial clays. *Transactions of the Japan Society of Civil Engineers,* 1955(30)**,** 1-92.

JABER, A., GORGIS, I. & HASSAN, M. Relationship between splitting tensile and compressive strengths for self-compacting concrete containing nano-and micro silica. MATEC Web of Conferences, 2018. EDP Sciences, 02013.

JAUBERTHIE, R., RENDELL, F., RANGEARD, D., et al. 2010. Stabilisation of estuarine silt with lime and/or cement. *Applied Clay Science,* 50(3)**,** 395-400.

JIANG, H., LI, Q., YANG, Z., et al. 2019. Experimental study on split tensile strength of glass fiber cement improved soil. *JOurnal of Railway Science and Engineering,* 16(11)**,** 2742-2747.

JIN, J., LI, J. & LI, X. 2014. Test ressearch on gypsum reinforced soft soil. *Architecture Technology,* 45(4)**,** 349-352.

KHOURY, N. N. & ZAMAN, M. M. 2002. Effect of wet-dry cycles on resilient modulus of class C coal fly ash-stabilized aggregate base. *Transportation research record,* 1787(1)**,** 13-21.

KOGBARA, R. B., AL-TABBAA, A., YI, Y., et al. 2013. Cement–fly ash stabilisation/solidification of contaminated soil: Performance properties and initiation of operating envelopes. *Applied Geochemistry,* 33(64-75.

KOLAY, P. & PUI, M. 2010. Peat stabilization using gypsum and fly ash. *Journal of Civil Engineering, Science and Technology,* 1(2)**,** 1-5.

KUMAR, A., WALIA, B. S. & BAJAJ, A. 2007. Influence of fly ash, lime, and polyester fibers on compaction and strength properties of expansive soil. *Journal of materials in civil engineering,* 19(3)**,** 242-248.

LAMBE, T. W. & WHITMAN, R. V. 1991. *Soil mechanics*, John Wiley & Sons.

LI, J., ZHU, X. & LIU, Y. 2010. Elasto-plastic damage constitutive model and its application to structural soft soil. *Journal of Zhejiang University （Engineering Science）,* 4(806-811.

LIANG, Y., LI, W. & WANG, X. 2013. Influence of water content on mechanical properties of improved clayey soil using steel slag. *Geotechnical and Geological Engineering,* 31(1)**,** 83-91.

LITTLE, D. N. & NAIR, S. 2009. Recommended practice for stabilization of subgrade soils and base materials.

LIU, J. & WANG, X. 2019. Study on size effect of splitting strength of cement stabilized laterite granules. *Highway & Transportation in inner Mongolia,* 173(5)**,** 13-18.

MATALUCCI, R., ABDEL-HADY, M. & SHELTON, J. 1970. Influence of microstructure of loess on triaxial shear strength. *Engineering Geology,* 4(4)**,** 341-351.

MAYNE, P. W. Stress-strain-strength-flow parameters from enhanced in-situ tests. Proc. Int. Conf. on In Situ Measurement of Soil Properties and Case Histories, Bali, 2001. 27-47.

MISHRA, P., DAS, D., UKAMANAL, M., et al. 2015. Multi-response optimization of process parameters using Taguchi method and grey relational analysis during turning AA 7075/SiC composite in dry and spray cooling environments. *International Journal of Industrial Engineering Computations,* 6(4)**,** 445-456.

MUNTOHAR, A. S. 2005. The influence of molding water content and lime content on the strength of stabilized soil with lime and rice husk ash. *Civil Engineering Dimension,* 7(1)**,** 1-5.

NATT, G. & JOSHI, R. 1984. Properties of cement and lime-fly ash stabilized aggregate.

Transportation Research Record, 998(32-40.

NICHOLSON, P. G., KASHYAP, V. & FUJII, C. F. 1994. Lime and fly ash admixture improvement of tropical Hawaiian soils. *Transportation Research Record,* 1440).

OUHADI, V., YONG, R., AMIRI, M., et al. 2014. Pozzolanic consolidation of stabilized soft clays. *Applied Clay Science,* 95(111-118.

PANDEY, A. & RABBANI, A. 2017. Soil stabilization using cement. *International journal of civil engineering and technology,* 8(6)**,** 316-322.

PARSONS, R. L. & MILBURN, J. P. 2003. Engineering behavior of stabilized soils. *Transportation Research Record,* 1837(1)**,** 20-29.

PETRY, T. M. & LITTLE, D. N. 2002. Review of stabilization of clays and expansive soils in pavements and lightly loaded structures—history, practice, and future. *Journal of materials in civil engineering,* 14(6)**,** 447-460.

PRUSINSKI, J. R. & BHATTACHARJA, S. 1999. Effectiveness of Portland cement and lime in stabilizing clay soils. *Transportation research record,* 1652(1)**,** 215-227.

PURWANTO, H., SETIOBUDI, A. & RUSTAM, R. 2020. Stabilization of soft clay soil using a gypsum plafond waste based on CBR testing. *INternational Journal of Scientific & Technology,* 9(2)**,** 963-968.

QIU, M.-Y. & YU, Y.-N. 2010. Analysis of influence depth for roads induced by vehicle load [J]. *Rock and Soil Mechanics,* 31(6)**,** 1822-1826.

SENOL, A., BIN-SHAFIQUE, M. S., EDIL, T., et al. Use of class C fly ash for stabilization of soft subgrade. Fifth international congress on advances in civil engineering, 2002. Istanbul Technical University Istanbul, Turkey, 25-27.

SHABJAREH, S. S., SOLTANI, F., HEIDARIPANAH, A., et al. 2014. Laboratory study of the effect of temperature on strength and strain-stress curve of lime-stabilized soil. *Bulletin Environment Pharmacoly Life Science,* 4(1)**,** 376-381.

SHERWOOD, P. 1993. *Soil stabilization with cement and lime*.

SHI, L. G., ZHANG, M. & CAO, P. 2011. Triaxial shear strength characteristics of lime-soil reinforced with polypropylene fiber inclusions. *Rock and Soil Mechanics,* 32(9)**,** 2721-2728.

SIVAPULLAIAH, P. & JHA, A. K. 2014. Gypsum induced strength behaviour of fly ash-lime stabilized expansive soil. *Geotechnical and Geological Engineering,* 32(5)**,** 1261-1273.

SMITH, R. & PRATT, D. 1983. A field study of in situ California bearing ratio and dynamic cone penetrometer testing for road subgrade investigations. *Australian Road Research,* 13(4).

SOBHAN, K., GONZALEZ, L. & REDDY, D. 2016. Durability of a pavement foundation made from recycled aggregate concrete subjected to cyclic wet–dry exposure and fatigue loading. *Materials and Structures,* 49(6)**,** 2271-2284.

SU, Y., LUO, Z. & LI, X. 2012. Gray correlation analysis method for cut-and-fill roadbed slope stability based on uniform experiment. *Rock and Soil Mechanics,* 33(8)**,** 2259-2264.

TANG, Y., MIYAZAKI, Y. & TSUCHIDA, T. 2001. Practices of reused dredgings by cement treatment. *Soils and Foundations,* 41(5)**,** 129-143.

TAŞTAN, E. O. 2005. *Stabilization of organic soils using fly ash.* University of Wisconsin--Madison.

TONG, Q. 2015. *Mechanical characteristics and mechanisms of dredeged silt solidified by fly ash and slag.* Hebei United University.

TOPP, G. C. & FERRE, P. 2002. The soil solution phase. *Methods of soil analysis: Part,* 4(417-1074.

VALLEJO, L. 1988. The brittle and ductile behavior of clay samples containing a crack under mixed mode loading. *Theoretical and applied fracture mechanics,* 10(1)**,** 73-78.

VENKATRAMAIAH, C. 1995. *Geotechnical engineering*, New Age International.

WANG, D. & XU, W. 2012. Research on strength and durability of sediments solidified with high volume fly ash. *Rock and Soil Mechanics,* 33(12)**,** 3659-3664.

WANG, D. & XU, W. 2013. Experimental study on long-term strength and deformation properties of solidified sediments. *JOurnal of Central South University: Science & Technology,* 1(332-339.

WANG, T., WENG, X., ZHANG, J., et al. 2017. Strength characteristics of fiber-reinforced sand under dry-wet cycles. *Journal of Railway Engineering,* 14(4)**,** 721-729.

WANG, Y., YIN, K.-L. & AN, G.-F. 2004. Grey correlation analysis of sensitive factors of landslide. *ROCK AND SOIL MECHANICS-WUHAN-,* 25(1; ISSU 90)**,** 91-93.

XU, M. 2015. *Study on influence factors of unconfined compressive strength of cement-soil.* Northwest Agriculture & Forestry University.

YARAGAL, S. C., KUMAR, B. C. & JITIN, C. 2020. Durability studies on ferrochrome slag as coarse aggregate in sustainable alkali activated slag/fly ash based concretes. *Sustainable Materials and Technologies,* 23(e00137.

YIN, P. & GONG, X. 2011. Present situation of dredged mud synthesizing utilization. *Energy Research and Management,* 4(17-20.

ZHANG, H., XIE, J., ZHU, W., et al. 2004a. Present Situation of Dredged Materials Dumping and the Study of Transforming Dredged Mud into Regenerative Resources Difficulties of Refuses Dumping in China Seas and Countermeasures to Deal with These Problems. *Marine Science Bulletin,* 23(6)**,** 54-60.

ZHANG, Q. 2013. *Study on the engineering and expansive properties of solidifed dredged sludge-phosphogypsum blends.* Kunming University of Science & Technology.

ZHANG, Y., DING, R. & MIU, L. 2004b. Test study on strength of mucky cement-soil. *Journal of Highway and Transportation Research and Development,* 21(11)**,** 27-29.

ZHANG, Y. & ZHANG, X. 2007. Grey correlation analysis between strength of slag cement and particle fractions of slag powder. *Cement and concrete composites,* 29(6)**,** 498-504.